Applied Energy 421 (2026) 128171

Contents lists available at ScienceDirect

Applied Energy

journal homepage: www.elsevier.com/locate/apen

In partnership with ESA

A system-level assessment of geological hydrogen storage, renewable generation and demand prediction for clean electricity pathways: A Great Britain case study

Zongtai Zhang [a], Joseph W. Brown [b], Andrew F. Crossland [a], Roderick C.I. MacKenzie [a], Stuart Jones [b], Christopher Groves [a,*]

[a] Department of Engineering, Durham University, South Road, Durham, DH1 3LE, United Kingdom
[b] Department of Earth Sciences, Durham University, South Road, Durham, DH1 3LE, United Kingdom

HIGHLIGHTS

- Geological hydrogen storage significantly reduces peak unabated gas needs.
- Storage limits can constrain hydrogen utilisation and increase hydrogen-not-stored due to storage saturation.
- Large geological storage enables full use of renewable surplus across weather variability.
- Accelerated hydrogen deployment improves adequacy more than faster renewable build-out.
- System reliability depends on coordinated scaling of electrolysis, storage, and H_2-to-power.

GRAPHICAL ABSTRACT

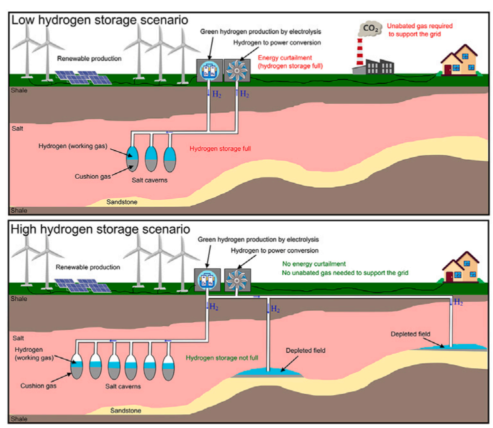

ARTICLE INFO

Keywords:
Renewable energy
Decarbonisation
Energy system
Electrolysis
Hydrogen storage
Unabated gas
Net-zero

ABSTRACT

High variable renewable energy (VRE) systems require flexibility that can maintain adequacy during multi-day renewable shortfalls while absorbing periods of surplus generation. This study evaluates the role of geological hydrogen storage in future Great Britain electricity pathways using a time-resolved dispatch model that combines historical half-hourly generation and demand data with National Energy System Operator (NESO) aligned capacity, storage and electrified-demand scenarios for 2030–2040. The model explicitly represents electrolysis, underground hydrogen storage, hydrogen storage losses and hydrogen-to-power dispatch, and compares baseline and accelerated deployment pathways. Results show that accelerated hydrogen deployment has a stronger adequacy benefit than accelerated renewable and battery deployment alone. In 2030, all acceleration pathways reduce the unabated gas generation share from 4.61% to approximately 1%. However, by 2040, accelerated hydrogen and electrolysis can reduce the remaining peak unabated gas requirement to zero, whereas accelerated renewables and batteries still leave approximately 15 GW. Hydrogen-system performance is strongly governed by storage availability. Under NESO and Low storage scenarios, storage saturation causes up to 60 TWh of hydrogen

* Corresponding author.
Email address: chris.groves@durham.ac.uk (C. Groves).

https://doi.org/10.1016/j.apenergy.2026.128171
Received 25 March 2026; Received in revised form 28 May 2026; Accepted 31 May 2026
Available online 15 June 2026

production to remain unstored in 2035 across pathways. In contrast, the High storage scenario eliminates hydrogen not stored due to storage saturation, and stored hydrogen can exceed 190 TWh by 2040. These results show that geological hydrogen storage can materially improve adequacy in high-VRE power systems, but only when electrolysis, storage inventory and hydrogen-to-power capacity are scaled as a coordinated flexibility chain. While quantified here for Great Britain, the results are directly relevant to other countries pursuing high-VRE pathways and subsurface hydrogen storage for seasonal balancing and net-zero electricity-system operation.

Nomenclature

Abbreviations

CCS	carbon capture and storage
CCUS	carbon capture, utilisation and storage
CNS	Central North Sea
DUKES	Digest of UK Energy Statistics
EV	electric vehicle
FES	Future Energy Scenarios
GB	Great Britain
IS	Irish Sea
LCOHS	levelised cost of hydrogen storage
LDES	long-duration energy storage
LHV	lower heating value
NESO	National Energy System Operator
NNS	Northern North Sea
PEM	Proton Exchange Membrane
PV	photovoltaic
SDS	short-duration storage
SI	Supplementary Information
SNS	Southern North Sea
SOC	state of charge
UHS	underground hydrogen storage
UK	United Kingdom
VRE	variable renewable energy

Units

GW	Gigawatt
GWh	Gigawatt-hour
TWh	Terawatt-hour

Symbols

s	different electrification demand sector
y	different scenario year
$d_y(t)$	the total electricity demand in scenario year y at time step t
$d_y^{\mathrm{base}}(t)$	the historical baseline demand in scenario year y at time step t
$d_{s,y}^{\mathrm{elec}}(t)$	the additional electrification demand from sector s in scenario year y at time step t
α_y	the scaling factor applied to the baseline demand component
D_y^{FES}	the annual electricity demand target from the NESO FES workbook in scenario year y
$D_{s,y}^{\mathrm{elec}}$	the annual additional electrification demand from sector s in scenario year y
D_y^{base}	the annual demand of the historical baseline year

1. Introduction

The United Kingdom (UK) has legislated and developed policy pathways for reaching net-zero greenhouse gas emissions by 2050, with the Net Zero Strategy setting out the role of power-sector decarbonisation in enabling wider emissions reductions across transport, buildings and industry [1]. This domestic trajectory is aligned with the broader international objective of limiting climate change under the Paris Agreement [2]. More recently, the Climate Change Committee's Seventh Carbon Budget has further emphasised the need for a largely decarbonised electricity system to support economy-wide electrification and net-zero delivery [3]. Delivering a net-zero electricity system requires not only the rapid scale-up of variable renewable energy (VRE) sources, particularly wind and solar power whose output depends on weather conditions, but also sufficient low-carbon flexibility to maintain system adequacy and operability across multiple timescales [4]. As VRE penetration increases, the capacity contribution of weather-dependent generation changes, reinforcing the need to assess adequacy and operability under high-renewable conditions [5]. As the share of these weather-dependent generation resources increases, system challenges shift from simply meeting annual energy demand to ensuring reliable supply during periods when wind and solar generation are simultaneously low while electricity demand remains high, while also managing periods of surplus generation under low-demand conditions, such as the "Summer Minimum" identified by National Energy System Operator's (NESO) Operability Strategy Report [6]. This increases the importance of storage, dispatchable low-carbon generation, and demand-side flexibility to balance both scarcity and surplus conditions. A growing body of evidence indicates that deeply decarbonised power systems require a portfolio of firm low-carbon resources, demand flexibility, interconnection and storage to manage residual demand across multiple timescales [7]. Long-duration storage (LDES) is particularly important for balancing multi-hour to multi-week variability in high-renewable systems [8], with its system value depending strongly on grid conditions, decarbonisation constraints and the availability of complementary flexibility options [9]. In the Great Britain (GB) context, flexible energy solutions are expected to play an important role in reducing reliance on residual fossil peaking capacity in a decarbonised power system [10].

High VRE penetration also induces periods of surplus generation in which curtailment becomes an economic and operational feature rather than an exception, and has increasingly been identified by NESO as an operability concern under future low-demand conditions. Curtailment can rise rapidly once flexibility options become saturated. Frew et al. describe this as a curtailment paradox in high-solar systems, where additional renewable capacity can produce diminishing marginal value without sufficient flexibility [11]. Law et al. further show that technological flexibility and grid coupling influence the extent to which hydrogen deployment can absorb renewable surplus in net-zero energy systems [12]. In practice, curtailment is not always fully controllable, particularly for distribution-connected generation that may not be directly visible or dispatchable by the system operator, further increasing operability challenges under surplus conditions [13]. These findings imply that net-zero pathways should be evaluated not only in terms of the annual energy mix, but also in terms of system operability, including whether flexibility portfolios can absorb surplus production and reliably re-dispatch it during scarcity periods without simply shifting constraints elsewhere.

This challenge is not unique to GB. Across the European Union, renewable sources accounted for 47.3% of electricity generation in 2025, indicating that high-renewable operation is already becoming a mainstream energy system condition [14]. The International Energy Agency further shows that several power systems, including the United Kingdom, Germany, Spain, Ireland, Denmark and Chile, are already operating, or are projected by 2030 to operate, at advanced phases of VRE integration, with VRE shares exceeding 50%, while China is approaching similarly high levels at around 40% [15]. In such systems, the central planning question is no longer only how to increase annual renewable generation [16], but how to manage multi-day to seasonal mismatch, curtailment, and residual firm-capacity requirements [17]. This has elevated long-duration and seasonal storage from a technology-specific challenge to a system-planning issue of broad international significance.

Hydrogen has consequently emerged as a strategic flexibility vector in net-zero pathways because it can couple low-cost renewable electricity to large-volume storage and dispatchable use in both the electricity sector and other energy applications [18]. Hydrogen can be produced from surplus electricity through electrolysis and subsequently provide dispatchable hydrogen-to-power generation during extended periods of supply shortfall [19]. Hydrogen can reduce whole-system decarbonisation costs and increase VRE utilisation when it is integrated as part of a wider flexibility portfolio. Lüth et al. show that electrolysis can provide flexibility in offshore energy-island systems [20], while van der Zwaan et al. demonstrate the role of electricity–hydrogen sector coupling in net-zero emission pathways [21]. However, the realised system value of hydrogen depends critically on the availability, performance and deliverability of hydrogen storage at scale, which ultimately determines whether surplus electricity can be converted and retained for later use or instead becomes curtailed electrolysis or stored hydrogen that cannot be effectively recycled.

Underground hydrogen storage (UHS) is widely considered as a key storage option capable of providing the large-scale, multi-week to seasonal period that could have a substantial impact on the adequacy of the national power system [22]. Comprehensive reviews describe the technical basis and remaining uncertainties of UHS, including barriers to deployment and the comparatively limited operational experience for hydrogen relative to natural gas storage [23]. For porous-media storage, including depleted fields and saline aquifers, Heinemann et al. highlight the scientific challenges associated with hydrogen storage at scale, including recovery, containment and reservoir behaviour [24]. Importantly, these geological storage classes differ in operational characteristics and in the mechanisms that can lead to hydrogen losses. In porous media, geochemical reactions, microbial consumption, mixing and trapping can reduce recoverable hydrogen or affect deliverability, and the literature documents substantial uncertainty in loss rates and their dependence on site conditions and operational regimes [25]. In contrast, salt caverns are typically associated with lower loss expectations but face constraints related to rock-salt permeability, solution mining requirements and mechanical behaviour [26], cyclic loading and unloading during repeated operation [27], and site availability in the GB geological context [28]. Emerging work further underscores that deployable UHS depends both on the availability of suitable geological formations and on practical constraints affecting how quickly storage projects can be developed. Assessing storage feasibility therefore requires explicit differentiation between salt-cavern potential [29] and broader UK underground hydrogen storage options, including depleted fields [30].

The international relevance of this issue is further reflected in the fact that countries with high or rapidly growing VRE penetration are actively pursuing hydrogen deployment and, in several cases, subsurface storage. Denmark's national strategy targets 4–6 GW of electrolysis capacity by 2030, indicating that hydrogen conversion infrastructure is already being positioned as part of broader high-renewable system development [31]. Germany's hydrogen storage demand has been projected to increase from 2–7 TWh in 2030 to 76–80 TWh by 2045, with salt caverns expected to play a central role [32]. However, the near-term electrolyser deployment remains slower than strategic ambition, suggesting that implementation pace may itself influence whether hydrogen systems become conversion or storage constrained [33]. Chile has also been widely recognised as one of the most promising locations for large-scale green hydrogen and hydrogen-derivatives production because of its exceptional solar and wind resources [34]. However, regulatory and institutional barriers remain important constraints on deployment, as discussed by Sepúlveda [35]. In China, electrolysis deployment has accelerated rapidly, reaching 3.5 GW in 2024 and accounting for approximately 70% of global installed capacity [36]. At the same time, large-scale geological storage is increasingly recognised as a key challenge for coupling hydrogen production with renewable generation, particularly where salt cavern storage is expected to support renewable integration [37]. Taken together, these examples show that the core issue is not country-specific geology alone, but how the timing and scale of electrolysis, storage and hydrogen-to-power capability shape system adequacy and renewable utilisation under high-VRE conditions. Great Britain is therefore examined here as a well-constrained case study from which more general planning insights can be derived.

Although hydrogen is increasingly included in energy transition pathways and system modelling studies, there remains a need for robust quantitative evidence on how hydrogen-based flexibility should be deployed to maintain power-system reliability under high renewable penetration. The UK government's Clean Energy Superpower Mission: Areas of Research Interest explicitly frames LDES performance and cost reduction as a priority research challenge, identifying hydrogen as a particularly promising vector for long-duration buffering and dispatchable power [38]. The report further emphasises that multi-week hydrogen storage could provide substantial system value, but that research and development are required to ensure the structural integrity and operational reliability of both geological and above-ground storage infrastructures. In parallel, the IEA Hydrogen TCP Task 42 Underground Hydrogen Storage Technology Monitoring Report recommends assessing the criticality of UHS for security and supply–demand balancing at both national and international scales, including a comprehensive analysis of societal costs and benefits across alternative transition scenarios [39]. Together, these assessments indicate a broader unresolved issue that extends beyond any single national context: the conditions under which hydrogen storage can materially enhance system adequacy, reduce renewable curtailment, and limit residual reliance on dispatchable fossil backup in high-VRE electricity systems, as well as the scale at which these benefits can be realised. Despite growing international interest in this issue, time-resolved and operationally explicit evidence in the public domain remains limited, particularly from studies that quantify how available hydrogen storage capacity interacts with electrolysis, renewable variability, and hydrogen-to-power conversion to shape system outcomes under weather-dependent operating conditions.

In this study, we address this gap through a time-resolved dispatch analysis of Great Britain as a policy-relevant and data-rich case study for high-renewable electricity systems. The modelling framework combines GB half-hourly historical operational data with NESO-aligned future energy system demand and capacity pathways for 2030–2040, together with an explicit representation of hydrogen power-system dynamics. This includes electrolysis, hydrogen storage state of charge (SOC), hydrogen-to-power conversion, and storage losses, all evaluated across hydrogen storage capacity variants that span policy-led assumptions and geological upper bounds. Future electricity demand used in this study includes additional loads arising from electrified heating, electric vehicles (EVs) and other sectoral electricity uses consistent with pathway assumptions. This framework also enables assessment of both renewable curtailment and the remaining requirement for dispatchable backup generation, particularly unabated gas capacity, under different scenarios. While internal transmission constraints are not explicitly modelled, geographical aspects of storage and generation deployment are considered to ensure that conclusions remain consistent with reasonable network and resource distributions.

This study makes three primary contributions. First, it develops a time-resolved dispatch modelling framework that integrates historical operational data with future generation, storage and electrified-demand pathways, explicitly representing hydrogen system dynamics within a high-renewable power system. Second, it assesses the role of available geological hydrogen storage resources by evaluating system performance across storage capacities spanning policy assumptions and estimated geological potential. Third, it examines how the scale and utilisation of hydrogen storage influence power-system decarbonisation pathways, including impacts on renewable curtailment, peak unabated gas capacity requirements and long-duration system adequacy. The remainder of the paper proceeds from scenario construction and dispatch modelling, through adequacy and storage saturation diagnostics, to a discussion of implications for GB power-system planning and the role of underground hydrogen storage in enabling deep power-sector decarbonisation.

2. Method

Fig. 1 summarises the modelling framework adopted in this study, linking historical generation data, scenario construction and time-resolved plant dispatch simulation to evaluate future GB electricity pathways. The framework integrates historical generation and demand data with scenario-based targets of generation capacity, sector-coupled demand and hydrogen storage availability, which are then processed through a time-resolved plant dispatch model representing renewable generation, short and long-duration storage, electrolysis, hydrogen storage and dispatchable low-carbon power. The resulting simulations provide half-hourly system operation data together with adequacy and energy-balancing metrics used throughout this study. The following sections describe each component of this framework in detail, including data processing, scenario construction, model formulation and performance assessment.

2.1. Future energy scenarios

The model described in the Section 2.2 requires energy generation and demand scenarios for the future grid. In this section, we describe how these scenarios are constructed. We adopted time-resolved GB generation by fuel type profiles from 2016 to 2022 published by ELEXON as the empirical baseline underpinning both generation and demand reconstruction [41]. Historical installed generation capacities were obtained from the UK Department for Energy Security and Net Zero Digest of UK Energy Statistics (DUKES), using annual plant capacity data for conventional generation technologies [42]. For rapidly expanding renewable technologies, including onshore wind, offshore wind and solar photovoltaic (PV), quarterly installed capacity statistics reported in DUKES were used to better capture capacity growth within each year and avoid bias arising from rapid deployment [43]. Because the ELEXON generation-by-fuel-type dataset underestimates distribution-connected renewable output, particularly embedded generation and wind farms which do not have operational meters, the offshore wind, onshore wind and solar generation profiles were further adjusted using historic embedded generation estimates published by NESO [44]. This adjustment ensures that the resulting VRE generation profiles preserve the observed intra-day and seasonal variability while more accurately representing total wind and solar generation in the GB power system.

Future electricity demand scenarios for 2030, 2035 and 2040 were constructed by augmenting an empirically observed demand profile with sector-specific electrification loads, followed by scaling to match the annual electricity demand targets reported in the NESO Future Energy Scenarios (FES) for each scenario year (Table 1) [45]. In this study, these FES annual demand values are used as scenario-alignment constraints rather than as formal validation benchmarks. They ensure that the constructed half-hourly demand series remains consistent with the total annual electricity demand assumed in the corresponding NESO pathway, while the temporal structure of demand is inherited from observed historical GB demand profiles. The baseline demand profile is therefore defined as the time-resolved electricity load observed in the selected historical weather year, and additional loads represent the incremental demand from end-use electrification.

No independent historical back-casting exercise is claimed in this study. Instead, historical observations are used as empirical temporal templates. Half-hourly demand and generation profiles from 2016–2022

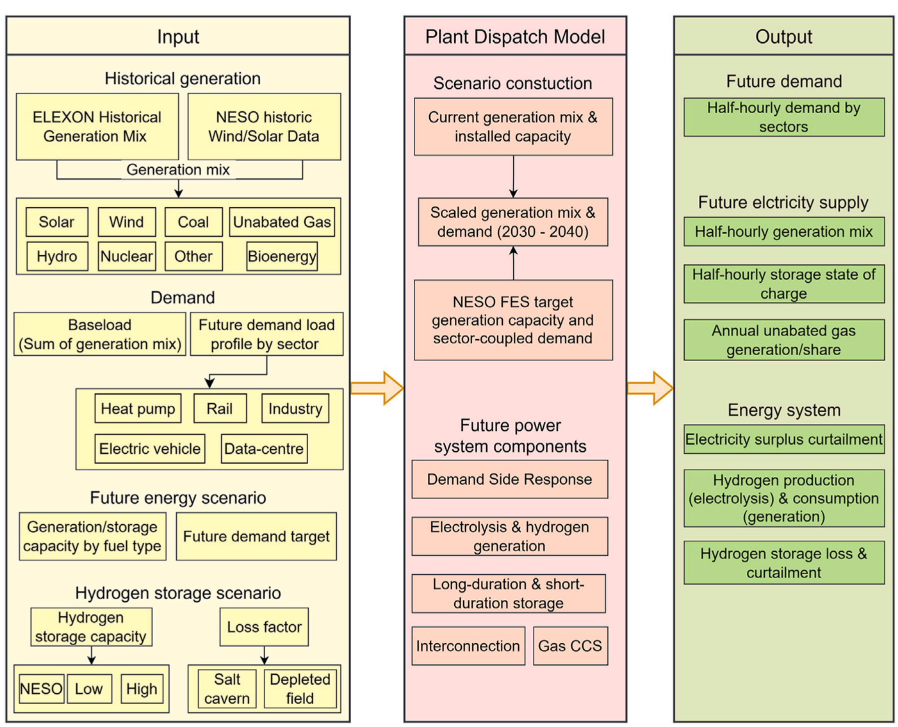

Fig. 1. Framework for future energy-scenario deployment and analysis.

Table 1
Installed generation, storage, and electrolysis capacities under the NESO hydrogen evolution pathway (2030–2040) [40].

NESO pathway	2030	2035	2040
Annual demand (TWh)	331.1	402.2	490.7
Capacity (GW)			
Unabated gas	36.0	23.8	16.3
Wind offshore	42.3	77.5	92.9
Wind onshore	27.3	35.8	38.9
Solar	43.3	55.7	68.5
Bioenergy	3.9	2.5	2.4
Hydro	1.9	1.9	2.0
Hydro pumped	3.0	6.0	6.0
Gas CCS	1.3	9.4	17.7
Hydrogen to power	0.05	7.1	17.8
Nuclear	2.9	5.0	6.0
Interconnection	11.7	17.9	17.9
Battery storage (GW/GWh)	20.5/29.0	24.8/33.0	28.3/38.0
LDES (GW/GWh)	3.0/30.0	7.5/96.0	9.2/103.0
Hydrogen storage (TWh)	1.99	12.05	25.06
Electrolysis (GW)	0.8	11.8	19.4

provide the chronology of demand, wind, solar and conventional generation variability, while future capacities and annual sectoral demands are imposed through scenario scaling. The model outputs should therefore be interpreted as internally consistent future operating simulations under specified NESO-aligned assumptions, rather than as a validated forecast of future GB system operation.

This explicit consideration of additional loads is a key element of our modelling of Net Zero pathways. Heat-pump electricity demand was constructed using the When2Heat dataset, which provides hourly weather-dependent heat-demand profiles and technology-specific coefficients of performance (COPs) for air-source, ground-source and water-source heat pumps for space-heating and domestic hot-water applications [46]. For each scenario year, the heat-demand profiles were converted into electricity demand using the corresponding COP assumptions and then scaled to the scenario-specific annual heat-pump electricity demand. This preserves the seasonal and intra-day structure of heating demand, including the strong winter concentration of heat pump load, while ensuring consistency with the adopted FES annual demand assumptions.

Residential EV charging demand was derived from the Element Energy and NESO EV charging profile dataset, which provides empirically based hourly charging profiles for GB domestic EV charging behaviour [47]. The normalised residential EV profile was scaled to the annual residential EV electricity consumption assumed in each scenario year. Commercial EV demand was treated separately and represented using standard normalised demand profiles from UK Power Networks, alongside the profiles used for rail, industry and data-centre electricity demand [48]. These sector-specific profiles were scaled to the corresponding annual sectoral electricity demands from the NESO FES demand data. Where necessary, hourly and half-hourly profiles were converted to the common model time step before being combined with the residual baseline demand profile. The resulting future demand series therefore combines an empirically observed residual baseline demand profile with explicit additional electrification components for heat pumps, residential EVs, commercial EVs, industry, rail and data centres.

The demand time series for each scenario year was obtained by combining a scaled residual baseline demand profile with additional sector-specific electrification components. The annual FES scenario demand target was imposed by scaling only the residual historical baseline demand component, rather than by applying a uniform correction to the total demand series after all electrification loads had been added. The final half-hourly demand series was therefore calculated as:

$$d_y(t) = \alpha_y d_y^{\text{base}}(t) + \sum_s d_{s,y}^{\text{elec}}(t),$$

where $d_y(t)$ is the total electricity demand in scenario year y, $d_y^{\text{base}}(t)$ is the historical baseline demand profile, $d_{s,y}^{\text{elec}}(t)$ is the additional electrification demand from sector s, and α_y is the scaling factor applied only to the baseline component. This factor was calculated as:

$$\alpha_y = \frac{D_y^{\text{FES}} - \sum_s D_{s,y}^{\text{elec}}}{D_y^{\text{base}}},$$

where D_y^{FES} is the annual electricity demand target from the NESO FES workbook, $\sum_s D_{s,y}^{\text{elec}}$ is the annual additional electrification demand from heat pumps, EVs, industry, rail and data centres, and D_y^{base} is the annual demand of the historical baseline year [40]. For the representative 2019 baseline used in the analysis, D_{2019}^{base} is 290.23 TWh. The resulting residual baseline adjustments are -19.62 TWh in 2030, -22.40 TWh in 2035 and -0.57 TWh in 2040, corresponding to baseline scaling factors α_{2019} of 0.932, 0.923 and 0.998, respectively.

This scaling changes the magnitude of the residual baseline component but does not alter the timing of its peaks, troughs or seasonal structure, because all half-hourly baseline values are multiplied by the same year-specific factor. The sector-specific electrification profiles are not rescaled after construction, so their temporal shapes and annual contributions are preserved. Adequacy metrics are therefore calculated from a half-hourly demand series that retains the chronological structure of both the historical baseline profile and the added electrification profiles, while remaining consistent with the annual FES demand target. The absolute peak residual demand, and hence the peak unabated gas capacity requirement, remains conditional on the adopted FES annual demand target and the baseline-component scaling described above.

Fig. 2(a) shows the demand composition in the 2035 scenario using the weather year 2019, where the scaled baseline demand is supplemented by electrified end-use sectors. Heat-pump demand exhibits strong seasonality, increasing winter electricity demand and contributing to periods of elevated system stress. EV charging introduces a relatively steady additional load throughout the year, while industrial, rail, and data-centre electricity consumption add smaller but persistent increments to overall demand. The grey half-hourly demand trace highlights substantial short-term variability around the rolling mean, underscoring the importance of flexibility resources capable of responding to intra-day fluctuations. Together, these patterns illustrate how electrification increases both total demand and temporal variability, reinforcing the need for dispatchable low-carbon generation and storage resources to maintain system adequacy under high VRE penetration.

2.2. Plant dispatch model

We now describe the model used to compute energy system outcomes based on future energy demand scenarios. To analyse adequacy and flexibility requirements in a future high-VRE GB power system, this study employed a time-resolved national scale dispatch framework capable of capturing dynamic changes in supply–demand balance under evolving generation and electrified demand structures. Unlike approaches focused primarily on annual energy balances, this framework explicitly resolves operational adequacy challenges arising during prolonged low-renewable periods and periods of elevated demand, allowing direct assessment of unabated gas peaking requirements, renewable curtailment, and hydrogen storage utilisation.

The modelling framework represents GB electricity supply–demand balancing using public datasets that enable chronological dispatch of conventional generation, variable renewable sources, low-carbon dispatchable generation, storage systems and electrolysis at hourly or half-hourly resolution. This approach has been used by Crossland et al. [49] to perform decarbonisation analysis in both New Zealand and the United Kingdom, and Williams et al. [50] to assess the impact of novel PV technologies on decarbonisation targets. In this study, the framework was substantially extended to represent future net-zero-aligned

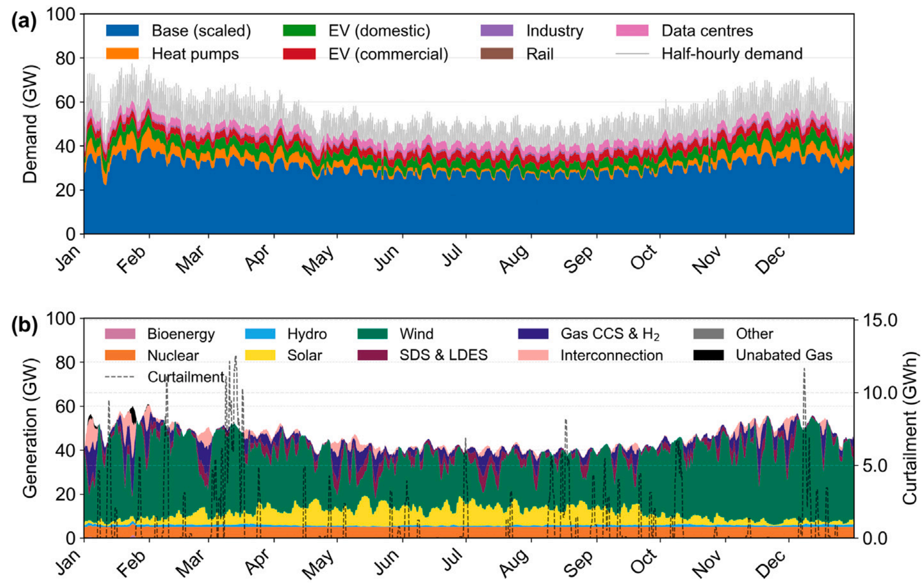

Fig. 2. Predicted daily average (a) demand composition in the 2035 scenario, including future electrified heat, transport, industry, rail, and data-centre loads; the grey line indicates half-hourly total demand. (b) Generation mix and curtailment in the same scenario, shown as a 24-hour rolling mean of half-hourly generation based on the weather year of 2019.

power-system operation by explicitly incorporating low-carbon flexibility resources and sector coupling to enable assessment of Net Zero pathways. From the perspective of generation and storage, we included low-carbon dispatchable generation (e.g., hydrogen-to-power and gas with carbon capture and storage (CCS)), interconnection, LDES and electrolysis capacity for power-to-hydrogen conversion with associated hydrogen storage.

The model is a time-resolved plant dispatch model in which technologies are prioritised according to dispatch class and representative carbon intensity. For each timestep, electricity demand is balanced using a fixed dispatch hierarchy organised by dispatch class. The dispatch classes distinguish inflexible generation, variable renewable generation, storage, low-carbon dispatchable generation, interconnection and residual fossil backup. Where several technologies are available within the same dispatch class, they are prioritised from lower to higher representative carbon intensity. Therefore, the model embeds a carbon-priority dispatch rule, but does not solve a formal carbon-minimisation objective function across all technologies and timesteps.

In each timestep, inflexible low-carbon generation is dispatched first, followed by available variable renewable generation. Residual demand is then met using short-duration storage (SDS), LDES, hydrogen-to-power generation and interconnection imports, subject to installed power capacities, SOC constraints and available energy inventories. Unabated gas is dispatched last and is interpreted as a residual adequacy metric, representing the remaining power requirement after the specified low-carbon generation, storage, hydrogen and interconnection resources have been used. During surplus periods, electricity first charges SDS and LDES, subject to their power and energy-capacity limits. The remaining surplus is then made available to electrolysis, subject to installed electrolyser capacity. Gross hydrogen production from electrolysis is subsequently compared with the available hydrogen storage headroom. The fraction that can be accommodated within the store is added to the hydrogen inventory, while any gross hydrogen production that exceeds the available storage headroom is recorded as hydrogen not stored due to storage saturation. This quantity is a hydrogen-storage-saturation diagnostic. Any further surplus is exported through electricity interconnection up to the export limit. Residual surplus beyond the available storage, electrolysis and export capacity is recorded as curtailed electricity. Therefore, this study distinguishes between electricity-side curtailment, which refers to surplus electricity that cannot be consumed, stored, converted to hydrogen or exported, and hydrogen-not-stored, which refers to gross electrolytic hydrogen production that cannot be retained because the geological hydrogen store is full.

Interconnection in the present model refers to electricity interconnection only. Hydrogen is modelled as a domestic power-sector flexibility vector, whereby surplus GB electricity is converted to hydrogen through electrolysis, stored in domestic geological hydrogen storage, and subsequently used for hydrogen-to-power generation within the GB electricity system. The model does not include hydrogen imports or exports, nor does it represent cross-border hydrogen pipeline or shipping constraints.

From a demand perspective, the model was expanded to include demand-side response from flexible electrified loads including heat pumps, EVs (commercial and domestic), as well as sector-specific loads including industry, data-centres and rail as described in Section 2.1. These additions enabled the model to capture operational interactions between storage, conversion technologies, and flexible demand, making it possible to diagnose when scarcity periods persist despite low annual unabated gas generation and when hydrogen storage saturation constrains system flexibility. Additional implementation details and equations are provided in the Supplementary Information (SI).

In the model, the Power-to-Hydrogen-to-Power cycle is represented as an explicit energy-conversion and storage chain linking surplus electricity, electrolysis, geological hydrogen storage and subsequent hydrogen-to-power generation. Surplus electricity remaining after direct demand, SDS charging and LDES charging is used as the available input to electrolysis, subject to installed electrolyser capacity and available hydrogen storage space. Electrolysis converts electricity into stored hydrogen on a lower heating value (LHV) basis using a fixed conversion efficiency of 70%. This value was selected as a representative system-level assumption consistent with efficiency ranges commonly reported for commercial alkaline and Proton Exchange Membrane (PEM) electrolysis systems in recent literature [51,52]. Reviews and techno-economic assessments indicate that practical electrolyser system efficiencies typically lie in the range of 60–80%, depending on technology type, operating conditions and system boundary definitions, with mid-range values commonly adopted for system modelling studies [53]. The full equations, including electrolysis limits, storage headroom, hydrogen inventory update, storage loss, hydrogen-to-power dispatch and hydrogen-not-stored calculation, are provided in the SI.

The hydrogen inventory is updated chronologically at each timestep according to hydrogen production, hydrogen withdrawal for power generation and storage losses. During scarcity periods, stored hydrogen can be withdrawn and converted back to electricity through hydrogen-to-power generation, subject to the installed hydrogen-to-power capacity and available hydrogen inventory. Hydrogen-to-power conversion is represented using an electrical efficiency of 60%, consistent with recent assessments of hydrogen utilisation in power generation [54]. Pashchenko reports that pure-hydrogen combined-cycle power plants can achieve electrical efficiencies approaching 60%, making this value an appropriate representation of high efficiency hydrogen low-carbon dispatchable generation within the modelling framework adopted here [55]. All efficiencies are applied on an LHV basis and represent aggregated system-level conversion performance at the model timestep, rather than component-level peak efficiencies. The resulting nominal electricity-hydrogen-electricity round-trip efficiency, excluding geological storage losses, is therefore 42%.

Consistent with a national-level representation, internal transmission constraints were not explicitly modelled. Instead, the system was treated as fully balanced at the GB aggregate level, implicitly assuming a reinforced transmission network without losses. This assumption is defensible given that high-voltage transmission losses in Great Britain are relatively small (1.5–2% of transmitted energy) [56,57]. This approach enabled the isolation of the impacts of flexibility technologies and operational strategies on national adequacy metrics. However, our results should be considered to be the best-case scenario.

Scenario-specific installed capacities were taken from the NESO FES capacity outlook for 2030–2040 in Table 1, and historical generation profiles were scaled to match these targets while preserving resource variability across 2016–2022 weather years set. As an example of this approach, Fig. 2(b) shows the predicted generation mix in the 2035 scenario based on the weather year of 2019, shown as a 24-hour rolling mean of half-hourly output. The aggregated GB wind and solar profiles already reflect geographic diversity across the system in 2019, and subsequent analyses consider multiple weather years to ensure robustness to interannual variability. SDS refers to battery storage. Wind generation provides the dominant share of supply throughout the year, with higher average output during winter months but also exhibiting substantial variability. Periods of low wind output still occur in winter, and when these coincide with seasonally reduced solar generation, system reliance on storage discharge, interconnection, and low-carbon dispatchable generation increases significantly. Solar generation contributes more strongly during spring and summer but declines substantially in winter, further tightening supply margins during low-wind periods and when electricity demand rises. Nuclear and bioenergy provide relatively stable output, with nuclear generation assumed to be fully available with the installed capacities specified in the NESO scenarios, while storage and interconnection operate dynamically to balance short-term mismatches between renewable supply and demand. The dashed curve in Fig. 2(b) additionally shows periods of renewable oversupply, represented as curtailed generation when available renewable output exceeds demand and available system flexibility. Curtailment occurs primarily during periods of high wind output combined with relatively low demand, indicating that surplus renewable generation cannot always be absorbed by storage charging, interconnection exports or electrolysis. Unabated gas generation appeared only intermittently in this analysis, primarily when low renewable availability coincides with elevated demand, illustrating its residual adequacy role rather than a significant contribution to annual energy supply.

The NESO FES presents several alternative pathways for the evolution of the GB energy system, reflecting different levels of electrification, consumer engagement and technology deployment [40]. These include pathways such as Electric Engagement, Falling Behind and Hydrogen Evolution, each representing distinct assumptions regarding the pace and structure of the energy transition. In this study, the Hydrogen Evolution pathway is adopted as the baseline scenario because it represents the most ambitious hydrogen deployment trajectory within the NESO framework. This pathway therefore provides an appropriate basis for assessing how large-scale hydrogen production, storage and hydrogen-to-power capacity may influence future power-system adequacy and renewable utilisation.

In addition to the NESO Hydrogen Evolution baseline pathway, three accelerated deployment pathways are considered to evaluate the system impacts of alternative investment sequencing. Each accelerated pathway is implemented as a five-year pull-forward of selected capacity trajectories from the NESO Hydrogen Evolution pathway: 2030 accelerated capacities are assigned from the 2035 baseline values, 2035 from 2040, and 2040 from 2045. This provides a consistent sensitivity test of earlier deployment while retaining the structure of the NESO pathway.

The accelerated hydrogen and electrolysis pathway advances electrolyser and hydrogen-to-power capacities by five years. The accelerated renewables and battery pathway advances offshore wind, onshore wind, solar PV and battery storage capacities by the same interval. The accelerated both pathway combines these two assumptions, such that electrolyser capacity, hydrogen-to-power generation, offshore wind, onshore wind, solar PV and battery storage are all advanced simultaneously using the same rule. All other installed capacities, demand assumptions, dispatch rules, storage efficiencies and hydrogen storage capacity scenarios are held constant relative to the NESO Hydrogen Evolution baseline for the corresponding model year.

The accelerated pathways are treated as controlled alternative cases for evaluating the effectiveness of hydrogen-enabled scheduling within the adopted dispatch framework. The NESO Hydrogen Evolution pathway provides the reference case, while the accelerated hydrogen and electrolysis pathway tests the effect of earlier deployment of hydrogen conversion and hydrogen-to-power capability. The accelerated renewables and battery pathway provides a non-hydrogen flexibility comparison, in which additional VRE and short-duration storage are prioritised instead. The accelerated both pathway tests whether coordinated expansion of renewable supply, electrolysis, hydrogen storage utilisation and hydrogen-to-power capacity provides additional system value beyond either single-technology acceleration. Because all other assumptions are held constant within each scenario year, differences in peak unabated gas requirement, annual unabated gas generation, renewable curtailment, electrolysis output, hydrogen-not-stored and storage SOC can be attributed to the alternative flexibility deployment strategies rather than to changes in demand, non-target technologies or dispatch assumptions.

2.3. Hydrogen storage

Considering the role of geological hydrogen storage in GB decarbonisation pathways is a key element of this paper. Hydrogen storage plays a central role in determining whether surplus renewable electricity can be retained and later dispatched to support system adequacy. To evaluate how storage availability influences grid operation, this study considers alternative assumptions regarding deployable hydrogen storage capacity in Great Britain. Three scenarios are therefore defined to compare policy-aligned deployment expectations with more ambitious storage availability scenarios.

Table 2 defines three scenarios: the NESO Hydrogen Evolution storage scenario, one more ambitious scenario, and one feasible hydrogen storage scenario based on estimates developed in this paper.

This study used these three storage scenarios within different pathways to model the impact of hydrogen storage capacity and hydrogen-to-power integration on the grid-scale energy system. This approach is similar to those previously applied to tidal energy generation [58]. The hydrogen storage capacities for the NESO Hydrogen Evolution pathway come from the NESO FES 2025 data workbook [40]. The other two scenarios, Low and High, are described as follows.

Table 2
Hydrogen storage capacities under the NESO and Low and High storage scenarios (2030–2040).

Hydrogen storage (TWh)	2030	2035	2040
NESO scenario [40]	1.99	12.05	25.06
Low scenario (this study)	4.13	9.05	15.55
High scenario (this study)	915.0	1827.0	3659.0

The Low scenario includes the gas capacity of hydrogen storage project proposals under development, as listed in Table 3. Each project has started development or is at the pre-application stage and has either a commercially reported completion date or a completion date estimated from published academic literature prior to its use in the model. The Rough field is treated as an exception because its future hydrogen-storage role remains uncertain. Wood has reported engineering work to assess the optimisation of hydrogen storage at Rough [59], while Centrica identifies Rough as part of its energy storage infrastructure portfolio [60]. In contrast, wider regional industrial-cluster assessments indicate that practical deployment depends on infrastructure, investment and system-integration constraints [61]. The field is also being reappraised in recent academic work focused on its geological suitability for underground hydrogen storage [62]. Table 3 reports the working-gas capacity of each project. For depleted gas fields, a 50% cushion-gas fraction was assumed. This assumption is consistent with studies examining cushion-gas requirements in hydrogen storage systems, including salt-cavern storage [63] and porous-media storage with alternative cushion gases [64]. The original gas capacities are taken directly from the literature and referenced in the table. The locations of these projects are shown in Fig. 3 to provide comparisons between the location of hydrogen storage sites and areas of highest wind curtailment.

The High scenario (Table 4), by contrast, assumes hydrogen storage capacities derived from the UK's available depleted offshore oil and gas fields (UK Hydrogen Storage Database) [65] and from potential new salt cavern storage capacities estimated in published UK geological assessments [29]. When we took the values directly from the UK Hydrogen Storage Database, we categorised this by region, summing the total storage capacities for the following regions: Southern North Sea (SNS), Northern North Sea (NNS), Central North Sea (CNS) and Irish Sea (IS). The fields already exist in varied states of operation and could be filled without geological modification [65], albeit with significant retrofitting/replacement of pipelines for transporting hydrogen safely or new well construction. By contrast, salt cavern storage requires solution mining to create the storage void space. While solution mining is a mature and commercially established technology, large-scale cavern development entails significant water consumption and generates substantial volumes of highly saline brine. Typical cavern construction requires multiple cubic metres of water per cubic metre of salt removed, and the resulting brine is often significantly more saline than seawater, which must be managed through offshore discharge under environmental regulation, deep geological reinjection, or limited industrial utilisation [66]. The scalability of these disposal pathways at the storage levels considered in the High scenario will be influenced by environmental permitting, infrastructure and water-resource constraints which may limit practical deployment rates.

Tables 3 and 4 list the total capacity available under different scenarios. In the following energy system modelling, it was necessary to assume a roll out of this capacity. The deployment of the Low scenario (Table 3) is based on projects currently under development, while the High scenario (Table 4) represents an upper-bound estimate of potential storage availability. Because no published source currently provides site-specific completion dates for the full set of depleted-field and salt-cavern resources included in the High scenario, we implemented the High scenario as a staged geological-availability sensitivity rather than as a forecast of project delivery. Specifically, we assumed that 25% of the total High scenario storage capacity is available in 2030, 50% in 2035 and 100% in 2040. These fractions provide a transparent interpolation between partial near-term access to the geological resource and full upper-bound availability by 2040, while recognising that practical deployment would be constrained by site conversion, solution mining, permitting, cushion-gas requirements, hydrogen transport infrastructure and project finance. We also assumed that there is 50% cushion gas fraction in all sites. This was chosen for the model input as a reasonable estimate based on a review of the literature, with [67] stating 50% cushion gas as an optimal ratio for underground hydrogen storage. The optimal value of cushion gas/working gas ratio depends on the cushion gas type, type of storage site and depth of site, but our 50% value serves as a reasonable yet conservative model assumption.

The High scenario should be interpreted as an upper-bound geological-potential case rather than as a proposed deployment target. Its purpose is to test the system behaviour when geological storage energy capacity is no longer the primary constraint. In this sense, the High scenario provides an effectively unconstrained storage benchmark against which the NESO and Low storage cases can be compared. Therefore, differences between the High and the lower-storage scenarios identify the effect of storage limits, while the remaining constraints observed within the High scenario indicate limitations arising from renewable-surplus availability, electrolysis capacity, hydrogen-to-power capacity, electricity demand and storage losses. Importantly, because the maximum simulated hydrogen SOC under the High scenario remains far below the imposed High storage capacity in all modelled years, the principal conclusions are not dependent on the precise 25% / 50% / 100% staging assumption once storage saturation has been removed.

In the model, we also accounted for hydrogen losses in the reservoir. Loss mechanisms reported in the literature include diffusion and solubility-driven migration, residual trapping within pore structures, abiotic geochemical reactions, mineral alteration and dissolution–precipitation processes [68], as well as microbial consumption in porous media reservoirs. The amount of loss varies widely in the literature as summarised in Table 5. All loss mechanisms occur in porous media (oil and gas reservoirs), whereas only some loss mechanisms are present in salt caverns. For example, residual trapping within pore spaces can only happen in a porous storage medium like a sandstone reservoir, whereas a salt cavern does not have this issue. The residual trapping loss mechanism is more difficult to generalise and quantify as it depends largely on

Table 3
Hydrogen storage projects under development in the Low hydrogen storage scenario (2030-2040).

Project	Capacity (TWh)	Storage type	Completion year	Reference
UKEn Dorset	3	Salt cavern	2035	ERA, 2025 [72,73]
UKEn East Yorkshire	1.2	Salt cavern	2035	ERA, 2025 [72,73]
Keuper Cheshire	1.3	Salt cavern	Assumed 2030	HIL, 2025 [74]
Teesside	0.03	Salt cavern	Completed	Jahanbakhsh et al., 2024 [30]
Rough	6.5	Depleted field	2040	Heinemann et al., 2025 [75]
MESH (East Irish Sea)	2.8	Salt cavern	2029	NS Energy, 2025 [76]
Aldbrough	0.32	Salt cavern	Assumed 2035	PI, 2024 [77]
Salinae	0.4	Salt cavern	2033	Uniper, 2025 [78]

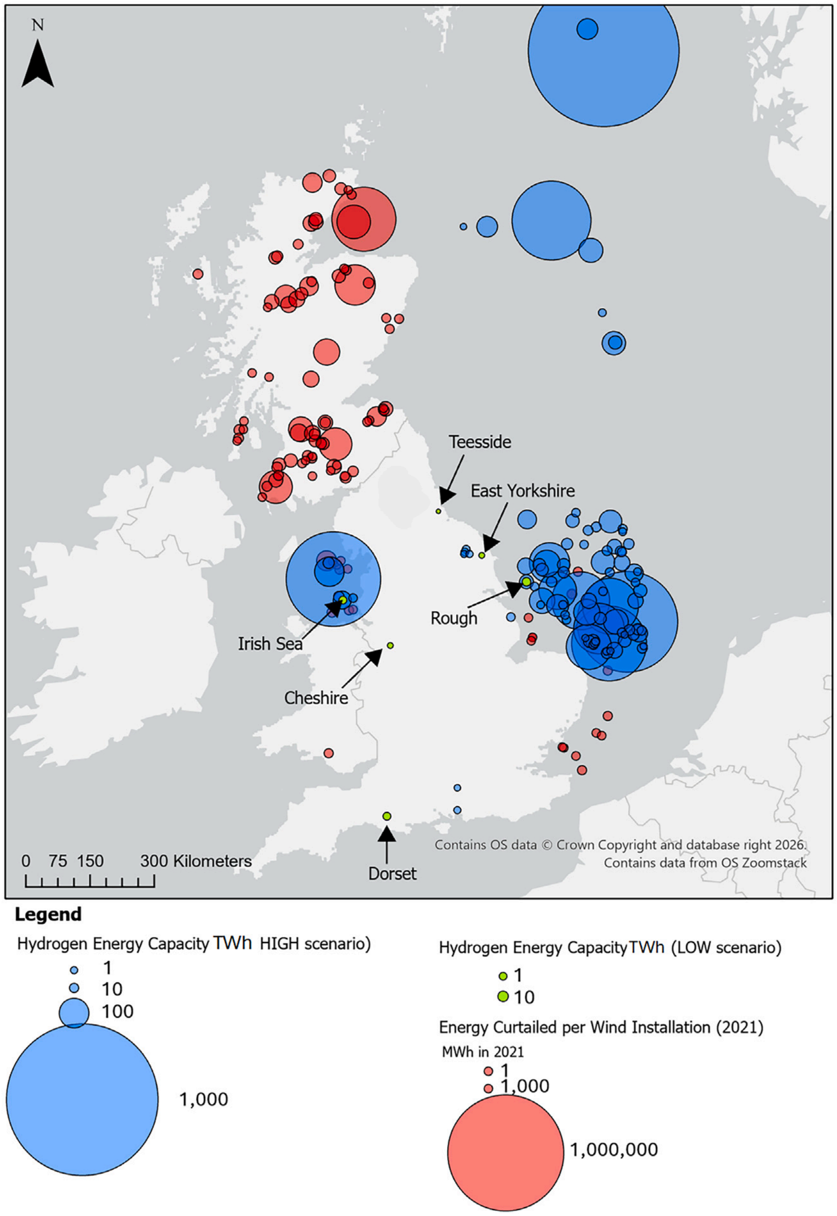

Fig. 3. Map of the locations of all hydrogen storage sites considered in the High scenario (blue circles) and in the Low scenario (green circles). The map also shows the locations of the highest energy curtailment by wind.

Table 4
Hydrogen storage calculations for the High scenario (2030–2040). IS = Irish Sea, SNS = Southern North Sea, CNS = Central North Sea, NNS = Northern North Sea.

Hydrogen storage capacity (TWh)	Location	2030	2035	2040
Depleted field	IS cluster	72	143	286
	SNS cluster	418	836	1672
	CNS cluster	77	154	309
	NNS cluster	79	157	315
Salt cavern	East Yorks	183	366	733
	Southwest	70	139	279
	Cheshire	16	32	65
Total	/	915	1827	3659

Table 5
Quantified hydrogen losses in underground hydrogen storage: examples of some estimates.

Loss Estimate	Quantified Loss	Source
Total	18% (one storage cycle)	Vahabzadeh et al., 2025 [70]
Geological loss (Diffusion)	0.1-5.5%	Perera, 2023; Vahabzadeh et al., 2025 [70,79]
Abiotic Loss	Negligible	Hassanpouryouzband et al., 2022 [80]
Biotic Loss	~4%	Vahabzadeh et al., 2025 [70]

the structure, pore-scale networks and permeability pathways as well as the well injection design. Literature on hydrogen loss shows high variability because the rates and magnitude of loss depend on specific site parameters such as temperature, pressure, salinity and mineralogy of the reservoir rocks. Taking into account this limitation, we made assumptions of the loss guided by the literature in Table 5. Presently, the most representative measure of loss over a season, including insertion and extraction losses, is 18% as measured in a depleted gas field in the Underground Sun Storage project [69,70]. It is expected that the loss in salt caverns would be much lower. Hence, in the energy system model, we assumed that depleted gas fields have 20% annual loss (on the upper end of the range), and a loss factor of 0% for salt caverns. The 0% value in salt caverns is consistent with estimates from recent literature where a loss estimate of 0.0007% is given [71].

For each storage scenario, the effective system-wide loss factor was determined by the fractional contribution of salt cavern and depleted field capacities within that scenario, with scenario-specific loss assumptions summarised in SI. The operational representation of hydrogen storage allows interaction with short-term system balancing rather than restricting storage to purely seasonal operation [80]. This operational assumption is supported by several strands of evidence. The HyPSTER project provides a European demonstration case for hydrogen storage in salt caverns [81]. Guan et al. further show that coordinated use of underground salt caverns and surface tanks can support more stable and scalable hydrogen supply under variable operating conditions [82].

Operational experience for depleted gas fields under high-frequency hydrogen cycling remains limited, and such reservoirs are generally expected to operate at seasonal or low cycle frequencies due to reservoir heterogeneity and uncertainty in hydrogen recovery behaviour [79]. In the present model, these uncertainties are represented through higher assumed storage loss factors in depleted-field-dominated scenarios, reflecting potential reductions in recoverable hydrogen rather than explicitly constraining injection or withdrawal rates.

3. Results

In this section, we analyse the NESO Hydrogen Evolution pathway as the baseline pathway alongside three accelerated deployment pathways: accelerated hydrogen and electrolysis, accelerated renewables and battery storage, and accelerated both hydrogen and renewables. These pathways use the five-year pull-forward mapping defined in Section 2.2, with all other assumptions held constant relative to the corresponding baseline year.

Fig. 4 presents the electricity supply mix under the NESO baseline pathway for weather year 2019 across the 2030–2040 period. Wind generation provides the dominant contribution to annual electricity supply and expands substantially over time, reflecting continued deployment of offshore and onshore wind capacity. Solar generation also increases across the period, while nuclear and bioenergy provide relatively stable contributions. Battery storage and long-duration storage deployment grow progressively, contributing to balancing renewable variability and reducing reliance on fossil generation. In addition, the figure illustrates the increasing role of hydrogen system operation through electrolysis losses and hydrogen generation losses. These losses arise from the conversion inefficiencies associated with electricity-to-hydrogen production via electrolysis and hydrogen-to-power generation during dispatch. As electrolyser capacity and hydrogen-to-power capacity expand over time, greater volumes of hydrogen are produced and subsequently utilised for power generation. Consequently, the absolute magnitude of these conversion losses increases across the modelling period, reflecting higher utilisation of hydrogen as a long-duration balancing resource within the system.

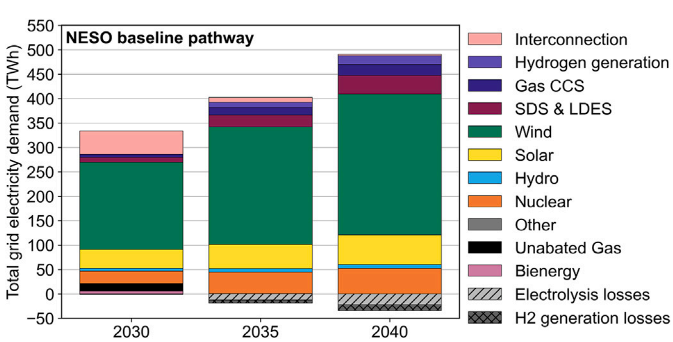

Fig. 4. Electricity mix under NESO baseline pathway (2030–2040) based on weather year 2019.

We then examine the performance of the pathways through the lens of unabated gas usage and curtailment, representing the effectiveness and efficiency of reaching net zero. The peak unabated gas capacity requirement is used here as a residual grid-adequacy metric. Annual unabated gas share indicates the residual energy still supplied by last-resort fossil generation, whereas the peak unabated gas capacity requirement indicates the power capacity required during the most stressed half-hour of the simulated year. This distinction is important in high-VRE systems because a scenario may have a low annual fossil generation share but still require substantial dispatchable capacity during short periods of coincident low renewable output, high electrified heat demand and limited stored energy availability.

Fig. 5 summarises the evolution of grid-level unabated gas dynamics across the baseline and accelerated pathways for 2030–2040, reporting peak unabated gas capacity requirements, annual unabated gas generation share, and wind curtailment. This comparison isolates the relative effects of accelerating hydrogen-system deployment, renewable and battery deployment, and their combined acceleration, thereby informing strategic decisions on future investment priorities. Despite the rapid expansion of low-carbon generation, unabated gas remains present in the 2030 NESO baseline pathway, primarily to meet residual demand during periods of low renewable output. By 2035 and 2040, annual unabated gas generation becomes much smaller, as hydrogen-to-power generation and gas with CCS provide increasing dispatchable low-carbon supply.

In 2030, all three accelerated pathways reduce the annual unabated gas share relative to the NESO baseline. The baseline unabated gas share is 4.61%, whereas both single-technology acceleration pathways reduce this value to approximately 1.3%, as shown in Fig. 5(a). Accelerated both pathway produces the largest reduction, because additional renewable generation reduces the residual energy requirement while expanded electrolysis and hydrogen-to-power capacity provide additional low-carbon dispatch during scarcity periods. A similar trend is observed in Fig. 5(b) for peak unabated gas capacity where all accelerated pathways reduce the peak requirement relative to the NESO baseline, with accelerated both pathway producing the lowest residual peak requirement in 2030. These results show that either accelerating hydrogen deployment or renewable and battery deployment can reduce fossil generation, but their combined deployment provides the strongest adequacy benefit.

Fig. 5(c) shows that the pathways differ more clearly in their curtailment behaviour. Accelerating renewables and batteries increases wind curtailment relative to the NESO baseline in 2030 and 2035, because additional wind output creates larger surplus periods that cannot always be absorbed by short-duration storage, interconnection or electrolysis. By contrast, accelerating hydrogen and electrolysis reduces wind curtailment relative to the baseline, because flexible electrolysis provides an additional sink for renewable surplus and converts part of this surplus into stored hydrogen for later dispatch. The accelerated both pathway exhibits the strongest trade-off. It combines the adequacy benefit of additional hydrogen-to-power capacity with the surplus generation effect of accelerated renewables. Consequently, it reduces unabated gas most strongly, but also increases wind curtailment in 2030 and 2035 because the renewable surplus increases faster than the system's ability to absorb, store and re-dispatch it. However, low wind curtailment in 2040 should not be interpreted as meaning that all surplus renewable electricity is converted into effectively stored hydrogen. The associated hydrogen system results in Figs. 7–9, which will be discussed later, showing that when geological hydrogen storage capacity is insufficient, part of the gross hydrogen production associated with electrolysis cannot be accommodated within the available storage headroom and is instead reported as hydrogen-not-stored due to storage saturation. In this situation, the binding constraint shifts from electricity-side wind

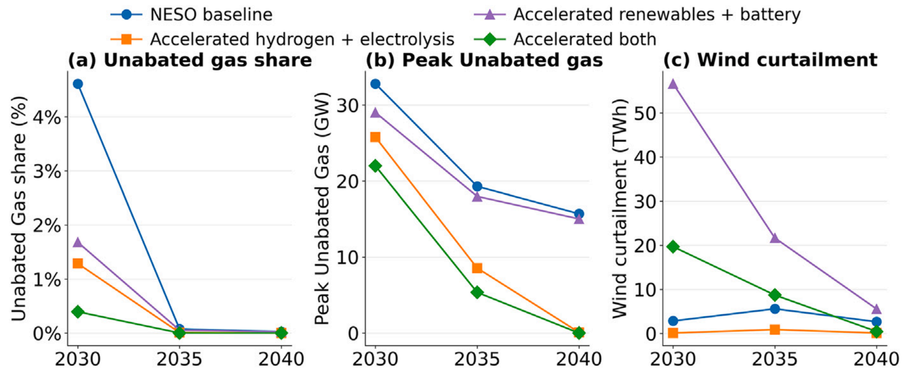

Fig. 5. Peak unabated gas demand, unabated gas generation share and wind curtailment under NESO baseline pathway and accelerated pathways (2030–2040) under weather year 2019.

curtailment to hydrogen-storage saturation. Therefore, the reduction in wind curtailment under the accelerated both pathway reflects improved electricity-side absorption of renewable surplus, but the final adequacy value of that surplus depends on whether the hydrogen storage has sufficient capacity to retain it for later dispatch.

By 2035 and 2040, the NESO baseline pathway grid system is nearly fully decarbonised, and the incremental reduction in annual unabated gas generation from acceleration becomes small, as shown in Fig. 5(a). However, the peak unabated gas requirement remains a more discriminating adequacy metric. The accelerated hydrogen and accelerated both pathways progressively suppress the remaining peak unabated gas requirement, reducing the residual peak from around 8 GW in 2035 to effectively zero by 2040. The accelerated renewables and battery pathway continues to reduce annual fossil generation but leaves a residual peak requirement of approximately 15 GW in 2040, reflecting the limited ability of SDS to cover multi-day renewable shortfalls.

Taken together, Fig. 5 shows that rapid renewable expansion mainly reduces annual fossil generation but can increase curtailment when system flexibility becomes saturated. In contrast, expanding hydrogen systems both lowers peak dependence on unabated gas and improves renewable utilisation by absorbing surplus generation. Shifting non-VRE supply away from a system dominated by unabated gas peaking towards dispatchable low-carbon hydrogen capacity, therefore improves system adequacy while reducing reliance on fossil fuel operations, with the additional benefit of lowering risk from future fuel price fluctuations.

We now turn our attention to how hydrogen is utilised in our simulated system. A consistent feature across all pathways is that increasing electrolysis capacity raises total hydrogen production, but the extent to which this hydrogen can be retained and utilised depends on available hydrogen storage capacity. Under the NESO and Low storage scenario, storage saturation occurs frequently under accelerated pathways, causing part of the hydrogen production to be recorded as hydrogen-not-stored, as shown in Fig. 6(a). However, these results also indicate that renewable surplus electricity is sufficient to rapidly build substantial hydrogen reserves, demonstrating that available geological storage can accumulate large energy reserves rather than merely acting as a short-term buffer.

Fig. 6(b) illustrates the evolution of hydrogen storage SOC during 2035 for two different initial SOC values of 0% and 50% in the NESO baseline pathway and storage scenario. The storage reservoir fills rapidly in both cases, reaching maximum capacity within a single simulation year regardless of initial storage level. This indicates that electrolysis capacity combined with renewable surplus in this scenario is sufficient to saturate available storage even when the reservoir is initially empty. Once storage approaches full capacity, additional hydrogen production cannot be retained, causing electrolysis output to be curtailed. Nevertheless, the rapid increase in SOC demonstrates that storage availability exceeds immediate power-sector requirements, implying

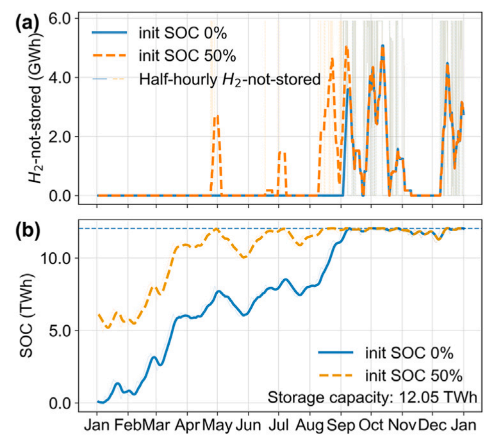

Fig. 6. Sensitivity of hydrogen storage dynamics to initial SOC in the NESO baseline pathway and hydrogen storage scenario for 2035 (weather year 2019). (a) Hydrogen not stored due to storage saturation. (b) Hydrogen storage SOC, shown as a 24-hour rolling average overlaid on the half-hourly series.

that additional hydrogen production could be directed to other energy uses or retained to improve resilience against adverse meteorological years.

Figs. 7–9 expands this analysis beyond a single representative weather year to present the evolution of key grid indicators for 2030, 2035 and 2040, respectively, under four pathways—NESO baseline, accelerated hydrogen & electrolysis, accelerated renewables & battery storage, and accelerated both hydrogen and renewables. Each pathway is evaluated for three hydrogen storage capacity scenarios: NESO, Low and High hydrogen storage scenarios. To investigate inter-year resilience, we simulate a run of 7 weather years in each case. Rather than applying the historical years 2016–2022 in chronological order, these analyses employ randomised sequences of the seven weather years (Y1 - Y7), with each simulation of scenario and pathway run three times to quantify variability and produce mean values with error bars, ensuring that conclusions do not rely on a single chosen weather year. The comparison illustrates how the roles of electrolysis and hydrogen storage shift as decarbonisation progresses from 2030 to 2040.

Fig. 7 shows predicted system behaviour for 2030 for 4 pathways (NESO baseline, accelerated hydrogen & electrolysis, accelerated renewables & battery storage, accelerated both) and 3 hydrogen storage scenarios (NESO, LOW, High). Across all pathways and scenarios in Fig. 7, electrolysis output shows substantial interannual variability, consistent with the strong dependence of renewable surplus availability on weather-year conditions. Under the 2030 baseline with the NESO and Low storage scenarios, electrolysis output is initially higher in the first

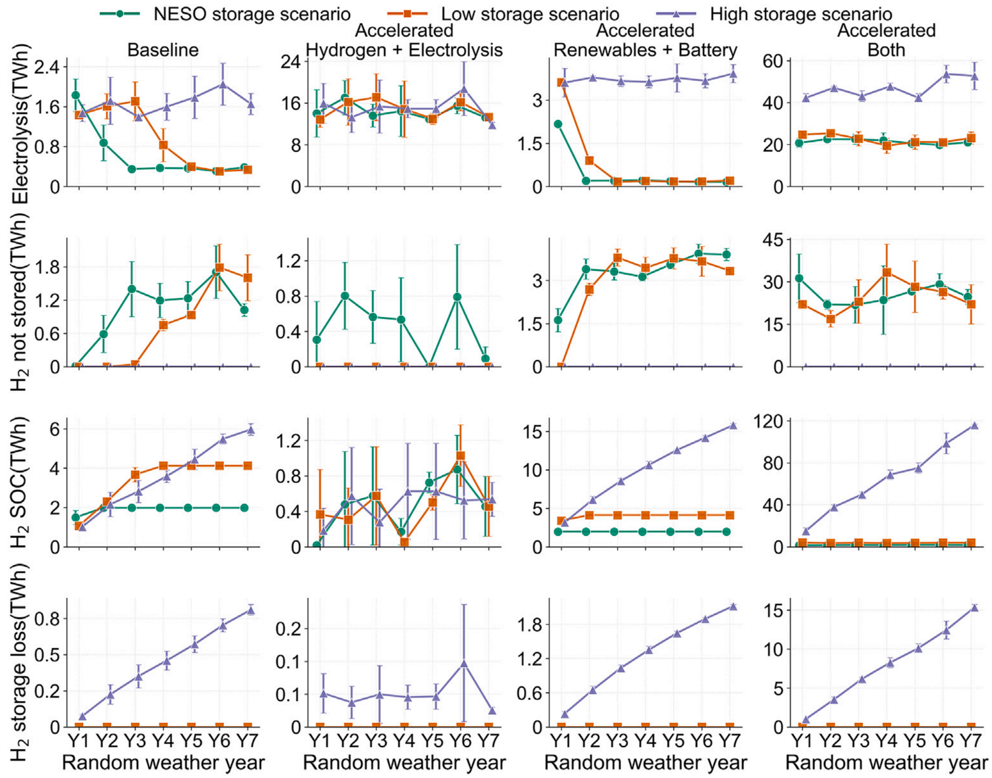

Fig. 7. Hydrogen-system indicators for 2030 across baseline and accelerated pathways.

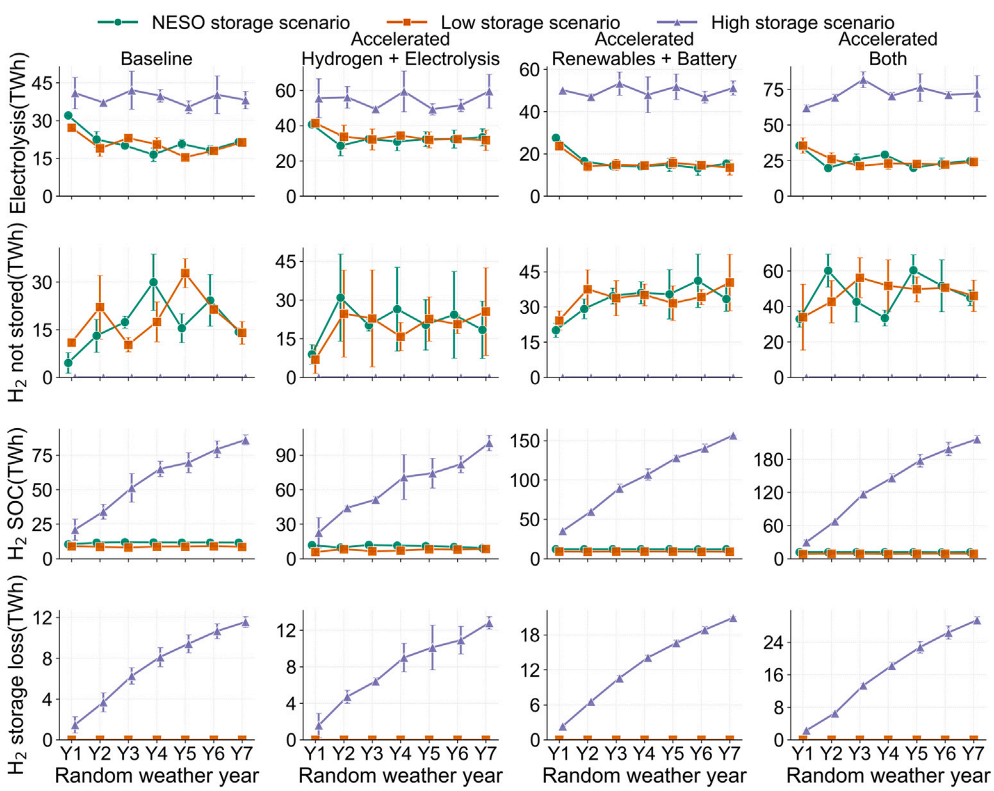

Fig. 8. Hydrogen-system indicators for 2035 across baseline and accelerated pathways.

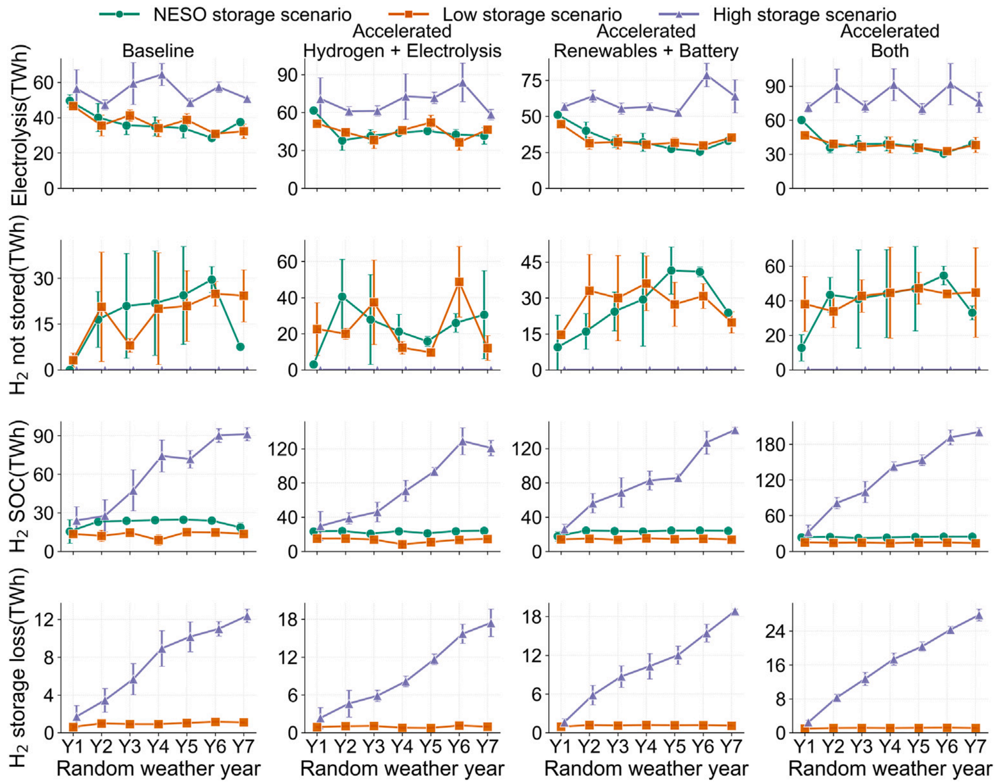

Fig. 9. Hydrogen-system indicators for 2040 across baseline and accelerated pathways.

simulation year, reaching around 1.6 TWh. However, once the storage reservoir approaches full capacity, electrolysis output declines to approximately 0.4 TWh in subsequent years, as additional hydrogen production cannot be retained and electrolysis operation becomes constrained by limited storage availability. However, in 2030, the system is not entirely storage-limited. In the baseline and accelerated renewables & battery pathways, electrolysis capacity remains relatively small, so hydrogen production itself is limited and only a small amount of renewable surplus can be converted to hydrogen. Accelerating hydrogen and electrolysis pathway increases electrolysis, reaching 10–24 TWh, while accelerating both hydrogen & electrolysis and renewables & batteries further raises electrolysis to 20–60 TWh, depending on the meteorological year and hydrogen storage capacity.

However, the three storage scenarios show different responses. In the NESO and Low scenarios, storage saturation occurs frequently under accelerated pathways, producing sustained hydrogen-not-stored. Hydrogen-not-stored remains limited in the baseline and accelerated renewables & battery pathways because electrolysis capacity in these pathways is relatively small, resulting in low hydrogen production. Consequently, the maximum hydrogen-not-stored reaches only around 1.8 TWh and 3.5 TWh, respectively. Although the accelerated hydrogen & electrolysis pathway substantially increases electrolysis output, it also expands hydrogen-to-power generation capacity. Under the 2030 system conditions, where renewable penetration remains comparatively low, a large fraction of the produced hydrogen is therefore consumed to supply electricity during periods of supply deficit. As a result, this pathway exhibits the lowest levels of hydrogen-not-stored, which is also reflected in the relatively lower average SOC across the simulation period. Storage generally accommodates most hydrogen, but accelerated both hydrogen and renewables pathway produces up to 45 TWh of hydrogen that cannot be stored, especially when the starting SOC is high. The hydrogen storage in the High scenario does not saturate for the pathways considered, with a maximum potential hydrogen storage around 120 TWh in 2030 pathways, allowing a larger share of electrolysis output to be retained and later converted via hydrogen-to-power generation. This result highlights that very large geological storage volumes can eliminate hydrogen not stored due to storage saturation and transform renewable surplus into firm long-duration flexibility.

Fig. 8 presents the corresponding results for 2035. Relative to the NESO baseline pathway, the accelerated hydrogen pathway increases electrolysis output by more than 10 TWh, with a further increase of around 20 TWh when both hydrogen and renewable deployment are accelerated. Compared with 2030, electrolysis output rises substantially across all pathways, reflecting both larger installed electrolysis capacity and greater renewable surplus available for conversion. As a result, the system in 2035 is much less constrained by conversion capacity than in 2030. Instead, the dominant limitation becomes storage capacity. Under the NESO and Low hydrogen storage scenarios, storage saturation occurs frequently, resulting in hydrogen-not-stored ranging from approximately 15 TWh to 60 TWh across pathways and weather-year realisations. In practice, hydrogen-not-stored means that electrolytic hydrogen production cannot be retained because available storage headroom has been exhausted. This reduces the effective flexibility value of electrolysis, even where electricity-side wind curtailment appears lower. By contrast, the High storage scenario provides sufficient capacity to store the additional hydrogen production and hydrogen-not-stored does not occur. At these high storage levels, storage losses become significant, reaching 25 TWh when stored hydrogen levels exceed 200 TWh in the High storage scenario under accelerated both hydrogen and renewables pathway. These results indicate that, by 2035, increasing electrolysis capacity alone does not increase the total amount of hydrogen stored when storage capacity is constrained. This highlights that hydrogen storage capacity becomes the key determinant of how much renewable surplus can be converted and stored.

Fig. 9 presents the corresponding results for 2040. Electrolysis output continues to increase under all the accelerated pathways relative to the baseline across all weather-year realisations, with the largest values occurring when both hydrogen and renewables deployment are accelerated. Storage behaviour is broadly similar to that observed in 2035. Under the NESO and Low hydrogen storage scenarios, storage saturation remains a persistent constraint, leading to continued hydrogen-not-stored events when hydrogen production exceeds available storage capacity. This indicates that by 2040, under limited storage scenarios, further expansion of electrolysis and renewable generation does not translate proportionally into additional stored hydrogen, because the system remains storage-limited.

By contrast, under the High storage scenario, hydrogen-not-stored does not occur, and maximum SOC reaches around 190 TWh in accelerated pathway for both hydrogen and renewables. This maximum SOC remains far below the imposed High storage capacity of 3659 TWh in 2040, confirming that the High scenario does not become geological storage energy-capacity limited. Instead, the remaining constraints under the High scenario arise from renewable-surplus availability, electrolysis capacity, hydrogen-to-power capacity, electricity demand and storage losses. At these high inventory levels, storage losses also become substantial. Overall, the 2040 results reinforce the 2035 finding that, once sufficient geological storage capacity is available, the dominant system challenge shifts from storage saturation to hydrogen inventory management, discharge capability and loss minimisation.

Taken together, Figs. 7 to 9 show that meteorological variability mainly influences the magnitude of electrolysis utilisation and hydrogen storage cycling, while comparative outcomes across pathways remain consistent. Across all weather-year realisations, hydrogen storage capacity and hydrogen-to-power capability determine whether additional electrolysis output can be effectively retained or instead leads to storage saturation and hydrogen-not-stored. This shows that the system benefit of accelerated hydrogen & electrolysis depends not only on hydrogen production capacity but also on sufficient storage and discharge capability to make effective use of surplus renewable energy.

Collectively, the time-domain results shown in Fig. 6 provide an operational explanation for the aggregate indicators for upcoming results of hydrogen-not-stored in Figs. 7–9. When hydrogen storage capacity becomes limiting, accelerated electrolysis deployment and renewable build-out shift the binding system constraint from electricity-side scarcity to hydrogen-side saturation. Under such conditions, additional electrolysis output cannot be effectively retained, leading to increasing hydrogen curtailment and reducing the marginal value of further electrolysis expansion unless hydrogen storage capacity and hydrogen-to-power capability are expanded accordingly.

4. Discussion

Our results show that reductions in annual unabated gas generation occur faster than reductions in the firm capacity required to maintain system adequacy. Although the share of unabated gas in total electricity supply declines rapidly, residual peaking capacity remains necessary to meet demand during multi-day periods of low renewable output. This study therefore provides an operationally explicit assessment of how hydrogen-enabled flexibility influences adequacy in a high-VRE future GB power system. The main finding is that the system impact of hydrogen is not determined by electrolysis capacity alone, but by the interaction between renewable surplus availability, hydrogen storage capacity, discharge capability, and geological storage loss characteristics. Hydrogen deployment becomes most consequential when it reduces peak unabated gas capacity requirements and diversifies backup supply beyond reliance on unabated gas, rather than simply lowering annual fossil generation shares. In this context, accelerating hydrogen deployment provides a clearer pathway for reducing peaking requirements than strategies dominated by renewable expansion and SDS, particularly in years where scarcity periods extend beyond typical battery discharge durations.

The results further indicate two distinct operational regimes. Firstly, hydrogen operates as an effective long-duration flexibility resource, where surplus electricity is converted via electrolysis, stored, and later dispatched through hydrogen-to-power generation during periods of supply scarcity. In the second regime, the hydrogen system becomes saturation-limited, where storage reaches full SOC during high-renewable periods, electrolysis is curtailed, and additional renewable build-out yields diminishing returns unless storage inventory increases commensurately. From an operational perspective, this saturation regime implies that pathway narratives which accelerate VRE and electrolysis without commensurate storage expansion risk shifting the binding constraint from electricity-side renewable curtailment to hydrogen-storage saturation, thereby constraining the adequacy value that hydrogen could otherwise deliver.

These contrasting operational regimes are strongly influenced by the assumed hydrogen storage capacity. In this study, the storage scenarios are grounded in an assessment of GB geological hydrogen storage resources, which forms a key element of the analysis. Under the NESO and Low storage scenarios, storage volumes are frequently insufficient to absorb additional hydrogen production during high-renewable periods, leading to repeated storage saturation and curtailed electrolysis output. As a result, further increases in electrolysis capacity or renewable deployment yield limited additional system benefit because surplus energy cannot be retained for later use. In contrast, the High storage scenario largely removes this constraint by providing sufficient inventory to accommodate surplus hydrogen production, allowing more renewable energy to be stored and later dispatched through hydrogen-to-power generation. As expected, under very large storage volumes, storage losses become increasingly relevant, shifting the operational limitation from storage saturation to inventory management and associated loss mechanisms. These results highlight that the adequacy contribution of hydrogen depends not only on production capacity but also on the scale and performance of available storage.

Although the High storage scenario indicates that GB possesses substantial subsurface storage capacity, practical deployment remains contingent on overcoming several significant technical, geological, regulatory and social barriers. Prior review work has shown that underground hydrogen storage development is constrained not only by reservoir suitability, but also by operational safety, legal and regulatory uncertainty and public acceptance [23]. In the GB context, the limited geographical distribution of suitable salt-bearing formations increases the relative importance of depleted gas fields as a large-scale storage option. However, depleted fields are also likely to involve greater uncertainty in hydrogen recovery, seasonal losses, geochemical interactions and cycling performance than salt caverns, implying that theoretical storage availability does not directly translate into equivalent near-term deployability. Accordingly, the large geological capacities considered here should be interpreted as a strategic subsurface resource, rather than an implementation pathway.

The present study should therefore be interpreted as an operational and physical feasibility assessment. Although the levelised cost of hydrogen storage (LCOHS) and capital expenditures value are central to practical deployment, large-scale underground hydrogen storage remains at an early stage of commercial development, and there is not yet a robust generic cost basis that can be applied uniformly across a national portfolio of salt caverns and depleted gas fields. Recent techno-economic studies show that the cost of underground hydrogen storage depends strongly on storage technology, storage scale and injection-withdrawal frequency. Huang et al. developed an LCOHS framework for depleted gas reservoirs, salt caverns and lined rock caverns, showing that storage scale and cycling frequency materially affect the resulting storage cost [83]. Similarly, Talukdar et al. assessed underground hydrogen storage in Europe and reported strongly site-specific capital costs, with different levelised costs for porous-media storage and salt caverns [84]. These findings indicate that a single generic LCOHS or capital expenditures value would not be sufficient for the mixed geological storage portfolio considered in this study. A robust economic assessment would require site-specific assumptions on cavern solution mining or depleted-field conversion, cushion-gas requirements, compression and purification systems, hydrogen-compatible wells and pipelines, injection and withdrawal deliverability, storage cycling frequency, asset lifetime, financing assumptions, operating costs and decommissioning. This work therefore motivates future integration of the dispatch framework developed here with a techno-economic storage module.

We discuss three limitations of the present work to contextualise the work and motivate further research. First, the model represents GB as a single node and does not explicitly capture internal transmission constraints. However, we have highlighted that the UK has specific regional clusters of potential hydrogen storage sites (Fig. 3) which create the possibility for the development of hydrogen hubs in these locations. This geographical constraint has the potential to benefit the local communities, providing reinvestment in these areas and local employment opportunities, but also creates a national energy system complexity that is beyond the scope of this study to model. We note that the development of hydrogen storage infrastructure may be complementary to emerging carbon capture, utilisation, and storage (CCUS) networks [85]. In Great Britain, several of the regions identified as suitable for large-scale hydrogen storage coincide with industrial decarbonisation clusters, where CO_2 transport and offshore storage infrastructure is also being developed. Such co-location may facilitate shared infrastructure, subsurface expertise, and coordinated investment in energy storage and carbon management systems. Second, the storage loss representation is stylised, intended to reflect geological-class uncertainty rather than site-specific reservoir simulations. However, this requires more research on hydrogen reservoir properties. Third, the analysis assumes hydrogen is primarily represented as a flexibility resource for electricity balancing. Competing hydrogen demands from industrial feedstocks, high-temperature heat or other non-power applications are not explicitly modelled here. Incorporating multi-sector hydrogen demand would likely further strengthen the importance of hydrogen reservoir capacity. These limitations motivate future work, including coupling spatial power-flow constraints with hydrogen transport and network constraints, and integrating site-resolved geological models to reduce uncertainty in storage performance and deliverability. Nonetheless, the comparison shows that NESO and Low storage assumptions remain storage-limited by 2040, whereas the High geological-potential case removes storage saturation and reveals the importance of conversion capacity, hydrogen-to-power capability and storage-loss management.

The international hydrogen fuel trade between GB and other European countries is not represented. The hydrogen storage requirements reported here should therefore be interpreted as domestic storage requirements under a no-hydrogen-trade assumption for power-system balancing. Hydrogen imports could reduce domestic storage requirements by providing dispatchable fuel during prolonged low-renewable periods, while hydrogen exports or competing European demand for hydrogen could increase the value of domestic geological storage and alter storage cycling behaviour. Capturing these effects would require a coupled representation of European hydrogen production, hydrogen transport infrastructure, import/export constraints, trade prices and non-power hydrogen demand. Such a multi-region formulation is beyond the scope of the present national plant dispatch model, but represents an important direction for future work.

The comparative analysis evaluates hydrogen-enabled scheduling across both deployment-pathway and storage-capacity scenarios within a rule-based plant dispatch framework. The pathway comparison distinguishes between accelerated hydrogen infrastructure, accelerated renewables and battery storage, and their coordinated deployment. The storage-capacity comparison further tests whether the benefits of hydrogen scheduling are limited by geological storage availability, using the NESO, Low and High storage scenarios. This two-dimensional comparison is appropriate for isolating the physical adequacy role of hydrogen storage, because the same dispatch logic is applied consistently across all pathways, storage scenarios and weather-year realisations. However, the comparison should not be interpreted as a claim that the adopted scheduling rule is globally optimal relative to all possible dispatch formulations. A full comparison with cost-minimising unit commitment, market-clearing models, stochastic optimisation, or alternative hydrogen storage-control heuristics would require additional assumptions on technology costs, bidding behaviour, reserve requirements, price formation, hydrogen transport constraints and operational limits on storage injection and withdrawal. Such optimisation-based comparisons are beyond the scope of the present national-scale adequacy analysis, but they represent an important direction for future work. In particular, future studies should compare rule-based hydrogen scheduling with optimisation-based dispatch and alternative storage control strategies, such as reserve-preserving SOC targets, seasonal hydrogen inventory targets, storage capacity dependent electrolysis limits and price-responsive electrolysis operation.

Although quantified here for Great Britain, the results are relevant to a broader class of high-renewable electricity systems. The central insight is that hydrogen's adequacy value is strongly regime-dependent. Systems with rapid VRE expansion but limited electrolysis remain conversion-limited; systems that scale electrolysis and VRE more rapidly than subsurface storage become storage-limited and experience rising curtailed electrolysis and diminishing returns from additional renewable build-out; only when electrolysis, storage inventory and hydrogen-to-power capacity are co-scaled does hydrogen act as effective long-duration and seasonal flexibility. The precise transition between regimes will vary across systems according to demand seasonality, interconnection, hydrology, existing low-carbon generation, and the availability and performance of geological storage resources. However, the underlying planning implications extend beyond Great Britain to other high-VRE systems pursuing subsurface hydrogen storage as part of wider decarbonisation strategies.

5. Conclusion

This study evaluates the role of hydrogen-enabled flexibility in future GB electricity pathways using time-resolved dispatch simulations that represent interactions between renewable generation, electrolysis, hydrogen storage and hydrogen-to-power generation. A key finding is that hydrogen contributes primarily by reducing peak unabated gas capacity requirements for grid adequacy, rather than by further lowering already small annual fossil generation shares. Although renewable expansion substantially reduces annual unabated gas generation, residual peaking capacity is still required to maintain system adequacy during periods of low renewable output. Our results indicate that hydrogen storage combined with hydrogen-to-power generation can reduce this peak unabated gas requirement by providing dispatchable low-carbon capacity during multi-day renewable shortfalls.

The analysis further shows that the system value of hydrogen is strongly governed by storage availability. When storage capacity is sufficient, renewable surplus can be retained and later dispatched to support system adequacy, whereas storage-constrained systems experience hydrogen-side saturation, limiting the benefit of additional electrolysis or renewable capacity. Large geological storage potential can largely remove this constraint, although storage losses become increasingly relevant at high inventory levels, as expected from the larger stored hydrogen volumes.

These findings imply that hydrogen should not be assessed as a standalone technology option, but as part of a coupled flexibility system in which renewables, electrolysis, storage and hydrogen-to-power capacity must be co-developed. For system planners, the key issue is therefore not only whether hydrogen is deployed, but whether the wider hydrogen chain is scaled in a coordinated manner such that material adequacy benefits can be realised. Although this study is parameterised for Great Britain, the planning logic is relevant to other high-renewable electricity systems considering subsurface hydrogen storage for long-duration and seasonal balancing.

CRediT authorship contribution statement

Zongtai Zhang: Writing – review & editing, Writing – original draft, Visualization, Validation, Software, Methodology, Investigation, Formal analysis, Data curation. **Joseph W. Brown:** Writing – review & editing, Writing – original draft, Visualization, Validation, Methodology, Investigation, Data curation. **Andrew F. Crossland:** Writing – review & editing, Validation, Supervision, Resources, Methodology, Investigation, Conceptualization. **Roderick C.I. MacKenzie:** Writing – review & editing, Visualization, Supervision. **Stuart Jones:** Writing – review & editing, Supervision, Resources, Methodology, Investigation, Conceptualization. **Christopher Groves:** Writing – review & editing, Visualization, Validation, Supervision, Project administration, Methodology, Investigation, Conceptualization.

Declaration of competing interest

The authors declare the following financial interests/personal relationships which may be considered as potential competing interests:

Joe Brown reports that financial support was provided by NeoEnergy Upstream. Andrew Crossland is employed by the National Energy System Operator (NESO) in GB. Contract from 2nd June 2025 to 1st June 2026. If there are other authors, they declare that they have no known competing financial interests or personal relationships that could have appeared to influence the work reported in this paper.

Acknowledgements

The authors acknowledge funding from Durham University through the Durham Engineering Doctoral Studentship and the GeoNetZero Centre for Doctoral Training (CDT). This work was conducted as part of a PhD within the CDT in Geoscience and the Low Carbon Energy Transition and was fully funded by NeoEnergy Upstream, whose support is gratefully acknowledged.

Appendix A. Supplementary data

Supplementary data to this article can be found online at doi:10.1016/j.apenergy.2026.128171.

Data availability

Data will be made available on request.

References

[1] Department for Energy Security and Net Zero and Department for Business, Energy & Industrial Strategy. Net zero strategy: build back greener. 2021. https://www.gov.uk/government/publications/net-zero-strategy [Accessed 24 January 2026].
[2] United Nations Framework Convention on Climate Change (UNFCCC). The Paris agreement (Nov, 2018. https://unfccc.int/sites/default/files/resource/parisagreement_publication.pdf., Publication; includes Decision 1/CP.21.
[3] Climate Change Committee. The seventh carbon budget. 2025. https://www.theccc.org.uk/publication/the-seventh-carbon-budget/ [accessed 12 August 2025]. Statutory report advising the UK Government on the carbon budget for 2038–2042.
[4] Sepulveda NA, Jenkins JD, De Sisternes FJ, Lester RK. The role of firm low-carbon electricity resources in deep decarbonization of power generation. Joule 2018;2(11):2403–20.
[5] Yu Y, Jiang H, Zhang N, Yong P, Teng F, Zhang J, Wang Y, Strbac G. Revisiting capacity value of variable renewable energy generation in power systems with high renewable energy penetration. J Mod Power Syst Clean Energy 2025;13(5):1593–603.
[6] National Energy System Operator (NESO). Operability strategy report. Tech. rep. National Energy System Operator; 2025 https://www.neso.energy/document/358121/download [Accessed: 12 February 2026].
[7] Jenkins JD, Sepulveda NA. Long-duration energy storage: a blueprint for research and innovation. Joule 2021;5(9):2241–6.
[8] Dowling JA, Rinaldi KZ, Ruggles TH, Davis SJ, Yuan M, Tong F, Lewis NS, Caldeira K. Role of long-duration energy storage in variable renewable electricity systems. Joule 2020;4(9):1907–28.
[9] Staadecker M, Szinai J, Sánchez-Pérez PA, Kurtz S, Hidalgo-Gonzalez P. The value of long-duration energy storage under various grid conditions in a zero-emissions future. Nat Commun 2024;15(1):9501.
[10] Xing H, Miles J, Scott S. Designing flexible energy solutions for a decarbonized GB power system. J Energy Storage 2026;152:120368.
[11] Frew B, Sergi B, Denholm P, Cole W, Gates N, Levie D, Margolis R. The curtailment paradox in the transition to high solar power systems. Joule 2021;5(5):1143–67.
[12] Law JW, Mignone BK, Mallapragada DS. Role of technology flexibility and grid coupling on hydrogen deployment in net-zero energy systems. Environ Sci Technol 2025;59(10):4974–88.
[13] Laimon M. Renewable energy curtailment: a problem or an opportunity? Results Eng 2025;26:104925.
[14] Eurostat. 47% of EU's electricity came from renewables in 2025. 2026. https://ec.europa.eu/eurostat/web/products-eurostat-news/w/ddn-20260319-2 [Accessed 22 March 2026]. Published: 19 March 2026.
[15] International Energy Agency. Integrating solar and wind: global experience and emerging challenges. 2024. https://www.iea.org/reports/integrating-solar-and-wind [Accessed: 22 March 2026].
[16] Ejuh Che E, Roland Abeng K, Iweh CD, Tsekouras GJ, Fopah-Lele A. The impact of integrating variable renewable energy sources into grid-connected power systems: challenges, mitigation strategies, and prospects. Energies 2025;18(3):689.
[17] Upadhyay A, Tröndle T, Ganter A, Petkov I, Gabrielli P, Sansavini G. The role of energy storage towards net-zero emissions in the European electricity system. Energy Convers Manag 2025;338:119887.
[18] He G, Mallapragada DS, Bose A, Heuberger-Austin CF, Gençer E. Sector coupling via hydrogen to lower the cost of energy system decarbonization. Energy Environ Sci 2021;14(9):4635–46.
[19] Gils HC, Gardian H, Schmugge J. Interaction of hydrogen infrastructures with other sector coupling options towards a zero-emission energy system in Germany. Renew Energy 2021;180:140–56.
[20] Lüth A, Werner Y, Egging-Bratseth R, Kazempour J. Electrolysis as a flexibility resource on energy Islands: the case of the North sea. Energy Policy 2024;185:113921.
[21] van der Zwaan B, Fattahi A, Dalla Longa F, Dekker M, van Vuuren D, Pietzcker R, Rodrigues R, Schreyer F, Huppmann D, Emmerling J, et al. Electricity-and hydrogen-driven energy system sector-coupling in net-zero CO_2 emission pathways. Nat Commun 2025;16(1):1368.
[22] Zivar D, Kumar S, Foroozesh J. Underground hydrogen storage: a comprehensive review. Int J Hydrog Energy 2021;46(45):23436–62.
[23] Tarkowski R, Uliasz-Misiak B. Towards underground hydrogen storage: a review of barriers. Renew Sustain Energy Rev 2022;162:112451.
[24] Heinemann N, Alcalde J, Miocic JM, Hangx SJ, Kallmeyer J, Ostertag-Henning C, Hassanpouryouzband A, Thaysen EM, Strobel GJ, Schmidt-Hattenberger C, et al. Enabling large-scale hydrogen storage in porous media–the scientific challenges. Energy Environ Sci 2021;14(2):853–64.
[25] Wu L, Hou Z-M, Luo Z-F, Fang Y-L, Huang L-C, Wu X-N, Chen Q-J, Wang Q-C. Impacts of microbial interactions on underground hydrogen storage in porous media: a comprehensive review of experimental, numerical, and field studies. Pet Sci 2024;21(6):4067–99.
[26] Grgic D, Al Sahyouni F, Golfier F, Moumni M, Schoumacker L. Evolution of gas permeability of rock Salt under different loading conditions and implications on the underground hydrogen storage in Salt caverns. Rock Mechanics and Rock Engineering 2022;55(2):691–714.
[27] Chang KW, Ross TS. Cyclic loading–unloading impacts on geomechanical stability of multiple Salt caverns for underground hydrogen storage. Int J Hydrog Energy 2025;102:767–77.
[28] Garvey C, Armitage T, Todd J, Noone M, Seakins J, Edlmann K. Revising the theoretical storage potential of hydrogen in UK Salt caverns: a multi-criteria assessment of the east coast of England. Geoenergy 2026;4(1). geoenergy2025–030.
[29] Williams JD, Williamson J, Parkes D, Evans DJ, Kirk KL, Sunny N, Hough E, Vosper H, Akhurst MC. Does the United Kingdom have sufficient geological storage capacity to support a hydrogen economy? Estimating the Salt cavern storage potential of bedded halite formations. J Energy Storage 2022;53:105109.
[30] Jahanbakhsh A, Potapov-Crighton AL, Mosallanezhad A, Kaloorazi NT, Maroto-Valer MM. Underground hydrogen storage: a UK perspective. Renew Sustain Energy Rev 2024;189:114001.
[31] European Hydrogen Observatory. Denmark: national hydrogen strategy. 2024. https://observatory.clean-hydrogen.europa.eu/hydrogen-landscape/policies-and-standards/national-strategies/denmark [Accessed: 22 March 2026]. Clean Hydrogen Joint Undertaking.
[32] Federal Ministry for Economic Affairs and Climate Action (BMWK). White paper on hydrogen storage (weißbuch wasserstoffspeicher). 2025. https://www.bundeswirtschaftsministerium.de/Redaktion/DE/Publikationen/Energie/weissbuch-wasserstoffspeicher-2025.pdf [Accessed: 22 March 2026].
[33] Institute of Energy Economics at the University of Cologne (EWI). Electrolysis ramp-up in Germany is proceeding slowly. 2026. https://www.ewi.uni-koeln.de/cms/wp-content/uploads/2026/01/20260120_PM_EWI-Analyse_Elektrolysehochlauf-in-Deutschland-verlaeuft-stockend-.pdf [Accessed: 22 March 2026]. Published: 20 January 2026.
[34] Rystad Energy. Chile's hydrogen vision: evaluating plans amid ambitious roadmap targets. 2024. https://www.rystadenergy.com/insights/chile-s-hydrogen-vision-evaluating-plans-amid-ambitious-roadmap-targets [Accessed: 22 March 2026].
[35] Sepúlveda E. Regulatory and institutional challenges to green hydrogen deployment in Chile. Int J Hydrog Energy 2026;224:154422.
[36] Fremery V, Yin Y, Hu N, Flickenschild J. China's hydrogen Sector 2025: balancing growth and challenges. Tech. rep. Sino-German Energy Partnership; Aug 2025 https://energypartnership.cn/publications-download-list/publications/chinas-hydrogen-sector-2025-balancing-growth-and-challenges/ [Accessed: 26 April 2026].
[37] Bai W, Shi X, Zhu S, Wei X, Huang Y. Opportunities and challenges of large-scale Salt cavern hydrogen storage in China coupled with renewable energy sources. Clean Energy 2025;9(1):179–96.

[38] Department for Energy Security and Net Zero. Clean energy superpower mission: areas of research interest. 2025. https://www.gov.uk/government/publications/clean-energy-superpower-mission-areas-of-research-interest [Online accessed 24 January 2026].
[39] IEA Hydrogen TCP Task 42. Underground hydrogen storage: technology monitoring report. Tech. rep. IEA Hydrogen Technology Collaboration Programme; 2023 https://filelist.tudelft.nl/Websections/H2%20platform/Task42_UHS_TechnologyMonitoringReport.pdf [Accessed 24 January 2026].
[40] National Energy System Operator. Future energy scenarios 2025 data workbook (version v006). 2025. https://www.neso.energy/publications/future-energy-scenarios-fes/fes-documents [Accessed: 4 March 2026].
[41] Elexon. Actual or estimated wind and solar power generation (AGWS/B1630). 2025. https://bmrs.elexon.co.uk/actual-or-estimated-wind-and-solar-power-generation [accessed 12 November 2025]. BMRS dataset page.
[42] Department for Energy Security and Net Zero. Electricity: Chapter 5, digest of United Kingdom energy statistics (DUKES). 2025. https://www.gov.uk/government/statistics/electricity-chapter-5-digest-of-united-kingdom-energy-statistics-dukes [Accessed: 16 February 2026].
[43] Department for Energy Security and Net Zero. Renewable sources of energy: Chapter 6, digest of United Kingdom energy statistics (DUKES). 2025. https://www.gov.uk/government/statistics/renewable-sources-of-energy-chapter-6-digest-of-united-kingdom-energy-statistics-dukes [Accessed: 16 February 2026].
[44] National Energy System Operator (NESO). Historic demand data. 2025. https://www.neso.energy/data-portal/historic-demand-data [accessed 12 November 2025]. NESO data portal—historic electricity demand and related datasets.
[45] National Energy System Operator (NESO). Electricity demand summary (ED1_2024). 2023. https://www.neso.energy/data-portal/fes-electricity-demand-summary-data-table-ed1/electricity_demand_summary_ed1_2024 [accessed 12 August 2025]. CSV data table of GB electricity demand summary for FES 2024.
[46] Ruhnau O, Hirth L, Praktiknjo A. Time series of heat demand and heat pump efficiency for energy system modeling. Sci Data 2019;6(1):189.
[47] Energy Networks Association. Development of GB electric vehicle charging profiles (project nia_ngso0021). 2019. https://smarter.energynetworks.org/projects/nia_ngso0021 [accessed 12 August 2025]. NIA project (Dec 2018–Jun 2019) producing GB EV charging profiles.
[48] UK Power Networks. Standard profiles UK power networks uses for electricity demand. 2025. https://ukpowernetworks.opendatasoft.com/explore/dataset/ukpn-standard-profiles-electricity-demand/information/ [accessed 12 August 2025]. Half-hourly load-factor demand profiles used in import curtailment assessments.
[49] Crossland A, Scoles K, Wang A, Groves C, Sun S. Assessment of electricity decarbonization scenarios for New Zealand and Great Britain using a plant dispatch and electrical energy storage modelling framework. Energies 2020;13(11):2799.
[50] Williams C, Michaels H, Crossland AF, Zhang Z, Shirshova N, MacKenzie RCI, Sun H, Kettle J, Freitag M, Groves C. Decarbonising electrical grids using photovoltaics with enhanced capacity factors. Energy Environ Sci 2023;16:4650–9.
[51] Buttler A, Spliethoff H. Current status of water electrolysis for energy storage, grid balancing and sector coupling via power-to-gas and power-to-liquids: a review. Renew Sustain Energy Rev 2018;82:2440–54.
[52] Yu Z-Y, Duan Y, Feng X-Y, Yu X, Gao M-R, Yu S-H. Clean and affordable hydrogen fuel from alkaline water splitting: past, recent progress, and future prospects. Adv Mater 2021;33(31):2007100.
[53] Aminaho EN, Aminaho NS, Aminaho F. Techno-economic assessments of electrolyzers for hydrogen production. Appl Energy 2025;399:126515.
[54] Venizelou V, Poullikkas A. The potential of green hydrogen as an alternative to natural gas power generation. Renew Sustain Energy Rev 2025;224:116028.
[55] Pashchenko D. Green hydrogen as a power plant fuel: what is energy efficiency from production to utilization? Renew Energy 2024;223:120033.
[56] Elexon Ltd. Transmission losses guidance. 2026. https://bscdocs.elexon.co.uk/guidance-notes/transmission-losses [Accessed: 13 February 2026].
[57] National Energy System Operator (NESO). Transmission losses. Tech. rep. National Energy System Operator; 2024 https://www.neso.energy/document/144711/download? [Accessed: 13 February 2026].
[58] National Energy System Operator (NESO). Strategic case for tidal range. Tech. rep. National Energy System Operator; 2025 https://www.neso.energy/document/370296/download [Accessed 24 January 2026].
[59] Wood plc. Wood to optimise hydrogen storage for centrica's rough field. 2024. https://www.woodplc.com/news/latest-press-releases/2024/wood-to-optimise-hydrogen-storage-for-centricas-rough-field [online accessed 24 January 2026].
[60] Centrica. Centrica energy storage (CES+) (rough). 2024. https://www.centrica.com/our-businesses/infrastructure/centrica-energy-storage-cesplus/ [online accessed 24 January 2026].
[61] Humber Industrial Cluster Plan. Economic impact summary 2023. 2023. https://www.humberindustrialclusterplan.org/files/Economic%20Impact%20Summary%202023.pdf [accessed 24 January 2026]. PDF.
[62] Brown JW, Knapp JL, Jones S, Gluyas J. A new investigation of the permian leman sandstone formation (LSF): suitability for underground hydrogen storage in the rough field, southern north sea, UK. Geoenergy 2026;4(1). geoenergy2025–035.
[63] San S, Karakilcik H, Karakilcik M, Erden M, Atiz A. Investigation of cushion gas/working gas ratios of underground Salt caverns for hydrogen storage. In: Emerging trends in energy storage systems and industrial applications. Elsevier; 2023. p. 67–78.
[64] Wang G, Pickup G, Sorbie K, Mackay E. Numerical modelling of H2 storage with cushion gas of CO_2 in subsurface porous media: filter effects of CO_2 solubility. Int J Hydrog Energy 2022;47(67):28956–68.
[65] Edlmann K, Armitage T, Slabon L, Thaysen E, Heinemann N, Mouli-Castillo J, Hemming C. UK hydrogen storage database. 2024. https://geosciences.ed.ac.uk/research/research-groups/edinburgh-earth-resources/uk-hydrogen-storage-database [accessed 26 November 2025]. [WWW Document]. University of Edinburgh.
[66] Qian X, You S, Wang R, Yue Y, Liao Q, Dai J, Tian S, Liu X. Underground hydrogen storage in Salt cavern: a review of advantages, challenges, and prospects. Sustainability 2025;17(13):5900.
[67] Viveros FE, Medina OE, Moncayo-Riascos I, Lysyy M, Benjumea PN, Cortés FB, Franco CA. Hydrogen storage in depleted gas reservoirs using methane cushion gas: an interfacial tension and pore scale study. J Energy Storage 2024;98:113110.
[68] Feng C, Jing Z, Li Y, Zhang Y, Liu Y. Hydrogen loss pathways in the process of underground hydrogen storage. Renew Sustain Energy Rev 2026;232:116835.
[69] RAG Austria AG. Underground sun storage project. 2026. https://www.rag-austria.at/en/innovation/innovation-projects/underground-sun-storage [Accessed: 13 February 2026].
[70] Vahabzadeh E, Hogeweg S, Nazari F, Hagemann B, Polya DA, Lloyd JR, Niasar V. Evaluating hydrogen loss in underground storage: the role of microbial activity, mixing, and operational strategies. Energy Fuels 2025;39(37):18112–27.
[71] Ghaedi M, Gholami R. Characterization and assessment of hydrogen leakage mechanisms in Salt caverns. Sci Rep 2025;15(1):185.
[72] Energy Research Accelerator (ERA). UKEn project overview. Tech. rep., PDF Energy Research Accelerator; 2025 https://www.era.ac.uk/wp-content/uploads/2025/05/UKEn-Project-Overview-Sheffield_Kris-Bone.pdf [accessed 24 January 2026].
[73] UK Energy Storage (UKEn). Project overview April 2025. Tech. rep., PDF UK Energy Storage; 2025 https://ukenergystorage.co.uk/wp-content/uploads/2025/04/Project-Overview-April-2025.pdf [accessed 24 January 2026].
[74] Hydrogen Industry Leaders. Costain secures pivotal role in Cheshire hydrogen storage megaproject. 2026. https://hydrogenindustryleaders.com/costain-secures-pivotal-role-in-cheshire-hydrogen-storage-megaproject/ [accessed 24 January 2026]. [online].
[75] Heinemann N, Edlmann K, Wilkinson M, Hassanpouryouzband A, Thaysen EM, Alcalde J, Haszeldine RS. Dynamic hydrogen working gas storage capacity in compartmentalised gas fields: the UK rough storage site as a case study. Int J Hydrog Energy 2025;140:45–54.
[76] NS Energy. Marram energy storage hub (MESH), UK. 2026. https://www.nsenergybusiness.com/projects/marram-energy-storage-hub-mesh-uk/ [online accessed 24 January 2026].
[77] Planning Inspectorate. EN030003. 2024. https://national-infrastructure-consenting.planninginspectorate.gov.uk/projects/EN030003 [online accessed 24 January 2026].
[78] Uniper. Salinae hydrogen storage project. 2025. https://www.uniper.energy/united-kingdom/projects-united-kingdom/salinae-hydrogen-storage-project [online accessed 24 January 2026].
[79] Perera M. A review of underground hydrogen storage in depleted gas reservoirs: insights into various rock-fluid interaction mechanisms and their impact on the process integrity. Fuel 2023;334:126677.
[80] Hassanpouryouzband A, Adie K, Cowen T, Thaysen EM, Heinemann N, Butler IB, Wilkinson M, Edlmann K. Geological hydrogen storage: geochemical reactivity of hydrogen with sandstone reservoirs. ACS Energy Lett 2022;7(7):2203–10.
[81] HyPSTER Project Consortium. HyPSTER: hydrogen pilot storage for large ecosystem replication, Fuel Cells and Hydrogen Joint Undertaking (FCH JU) Project, European Union. Available at: https://hypster-project.eu, 2023.
[82] Guan C, Wang Z, Deng H, Li S, Pan S, Li Z. Coordinated hydrogen storage strategy: integrating underground Salt caverns and surface tanks for stable and scalable hydrogen supply. Fuel 2026;406:137010.
[83] Huang Y, Shi X, Zhu S, Wei X, Bai W, Li P, Xu M, Li Y, Yang C. Comparative techno-economic analysis of large-scale underground hydrogen storage. Appl Energy 2025;400:126564. https://doi.org/10.1016/j.apenergy.2025.126564
[84] Talukdar M, Blum P, Heinemann N, Miocic J. Techno-economic analysis of underground hydrogen storage in Europe. iScience 2023;27(1):108771. https://doi.org/10.1016/j.isci.2023.108771
[85] Lu H, Xi D, Cheng YF. Hydrogen production in integration with CCUS: a realistic strategy towards net zero. Energy 2025;315:134398.